frontiers in Chemical Engineering

TYPE Original Research
PUBLISHED 30 March 2026
DOI 10.3389/fceng.2026.1791044

Check for updates

OPEN ACCESS

EDITED BY
Chang Geun Yoo,
SUNY College of Environmental Science and Forestry, United States

REVIEWED BY
Daehwan Kim,
Hood College, United States
Jiae Ryu,
SUNY College of Environmental Science and Forestry, United States

*CORRESPONDENCE
Niclas Conen,
n.conen@fz-juelich.de

RECEIVED 19 January 2026
REVISED 23 February 2026
ACCEPTED 02 March 2026
PUBLISHED 30 March 2026

CITATION
Choo H, Conen N, Doeker M, Pude R, Klose H and Jupke A (2026) Optimization of alkali-ethanol fractionation of *Miscanthus* using response surface methodology.
Front. Chem. Eng. 8:1791044.
doi: 10.3389/fceng.2026.1791044

COPYRIGHT
© 2026 Choo, Conen, Doeker, Pude, Klose and Jupke. This is an open-access article distributed under the terms of the Creative Commons Attribution License (CC BY). The use, distribution or reproduction in other forums is permitted, provided the original author(s) and the copyright owner(s) are credited and that the original publication in this journal is cited, in accordance with accepted academic practice. No use, distribution or reproduction is permitted which does not comply with these terms.

Optimization of alkali-ethanol fractionation of *Miscanthus* using response surface methodology

Halim Choo[1,2,3], Niclas Conen[1,2]*, Moritz Doeker[1], Ralf Pude[2,4], Holger Klose[1,2,3] and Andreas Jupke[1,2,5]

[1]Institute of Bio, and Geosciences, IBG-2: Plant Sciences, Forschungszentrum Jülich GmbH, Jülich, Germany, [2]Bioeconomy Science Center (BioSC), Jülich, Germany, [3]RWTH Aachen University, Aachen, Germany, [4]Institute of Crop Science and Resource Conservation, Faculty of Agriculture, University of Bonn, Rheinbach, Germany, [5]Institute of Fluid Process Engineering, RWTH Aachen University, Aachen, Germany

To address the demand for sustainable, sulfur-free fractionation, this study investigated the alkali-ethanol fractionation of *Miscanthus* × *giganteus* using sequential Response Surface Methodology (RSM) strategy to systematically quantify parameter interactions and optimize process performance. An initial Box-Behnken Design (BBD) was employed at low severity to screen four independent variables (temperature, time, alkali concentration and ethanol concentration), regarding their impact on pulp yield, pulp chemical composition, and xylan solubilization. Subsequently, a Central Composite Design (CCD) was used to optimize the principal process drivers (temperature and alkali concentration) at high severity. In both designs, distinct optima were identified for two specific objectives: maximizing polysaccharide yield and maximizing delignification. In the low severity regime, the predicted optimum for maximizing polysaccharide retention yielded a 73.3% pulp yield (96.9% cellulose and 92.2% xylan retention), while the delignification focused optimum achieved 83.1% lignin removal. In the high severity regime, maximizing polysaccharide yield resulted in 88.2% cellulose and 67.6% xylan retention, whereas delignification objective achieved 91.3% lignin removal. Chemical and morphological analyses confirmed that varying severity regimes and objectives produce pulps with distinct structural chemotypes. This study establishes a robust sequential RSM model that serves as a powerful tool for precisely tailoring non-wood feedstock fractionation, enabling biorefineries to switch between high yield intermediate pulps and high-purity cellulose streams based on specific market requirements.

KEYWORDS
alkali-ethanol, biomass, Miscanthus, process optimization, rsm, soda-ethanol

1 Introduction

Global paper and paperboard consumption reached 401 Mt in 2023, and is projected to grow to 476 Mt by 2030, primarily due to increasing demand for packaging and tissue products (Food and Agriculture Organization of the United Nations, 2024). Such demand has long been met primarily through pulp production using wood resources, which account for over 90% of global pulp production (Li et al., 2023). Demands on increased sustainability and resource availability have therefore drawn attention to the potential of non-wood biomass as an alternative raw material. As fiber quality strongly determines the quality of the end products, manufacturers are

increasingly exploring alternative fibers and adopting more sustainable sourcing strategies.

Among the promising candidates, *Miscanthus* species have attracted special attention as potential non-wood feedstocks for use not only in conventional pulp and paper making, but also in production of energy and construction material (Moll et al., 2020). As a perennial C4 grass, it offers a high carbohydrate content and wide ecological adaptability, as well as high biomass yields (up to 20 Mg/ha) (Lee and Kuan, 2015; Clifton-Brown et al., 2017; Danielewicz and Surma-Ślusarska, 2019), making it an attractive feedstock for diverse biorefinery applications (Moll et al., 2020). Furthermore, Miscanthus is recognized as strategic model crop for the European bioeconomy due to its high carbon fixation rates while requiring low nutrient and water inputs, making it ideal for large-scale production on marginal lands in alignment with the EU Bioeconomy Strategy and the European Green Deal (Ben Fradj et al., 2020; Shepherd et al., 2023).

Beyond its ecological adaptability, *Miscanthus* × *giganteus* is characterized by considerable high cellulose content and moderate lignin content compared to other common agricultural residues. For instance, while wheat straw typically contains 33%–38% cellulose and 17%–19% lignin content, switchgrass exhibits a lower cellulose content (5%–20%) alongside higher lignin content (10%–40%) (Tayyab, 2018). The chemical composition of *Miscanthus* × *giganteus* has been shown to vary with environmental factors. Gismatulina et al. reported ranges of 43.2%–55% for cellulose and 17.1%–25.1% lignin across different climatic regions in Russia (Gismatulina et al., 2022). Additionally, the lignin architecture of *Miscanthus* × *giganteus* is particularly advantageous for fractionation, as it features a higher density of the labile β-O-4 linkages (82%) and a syringyl-to-guaiacyl (S/G) ratio of 0.7–0.9 (Wang et al., 2012; Bergs et al., 2020) compared to those found in other grass lignins, such as sugarcane bagasse (0.09–0.22) (Xu et al., 2020), which further supports the potential for efficient structural disruption and the recovery of high-purity components.

Alkaline fractionation is a widely used chemical treatment method which involves the use of alkali/alkaline solutions to enhance the solubilization of lignin by reducing the degree of polymerization through the cleavage of α- and β-ether bonds and breaking the bond between lignin and carbohydrates (Takada et al., 2020). The most widespread alkaline process is Kraft pulping, which is the dominant chemical pulping process at an industrial scale. It is mainly used due to its short pulping periods, high yields, and recovery of pulping chemicals, although environmental issues have been caused by the presence of sulfur (Imlauer Vedoya et al., 2022). As an alternative to this conventional method, many researchers have attempted to explore different fractionation processes, such as soda, soda-AQ and organosolv *etc.* Alkaline-ethanol fractionation, also referred to as ethanol-soda pulping, is also one of the alternatives to conventional pulping. This approach is particularly promising, as the addition of ethanol to the alkaline solution enhances polysaccharides preservation against degradation and improves the selectivity of delignification, resulting in higher yields and quality of pulp (Shatalov and Pereira, 2004; Berhanu et al., 2018; Imlauer Vedoya et al., 2022). Alkaline-ethanol pretreatment has been applied to a wide range of lignocellulosic biomass, and studies have shown that the reaction conditions and effects of individual operating variables strongly depend on the chemical and structural features of the raw materials. This underscores the need for targeted investigations of operating variables and the corresponding process optimization (Carvalho et al., 2014; Dagnino et al., 2017; Berhanu et al., 2018; Imlauer Vedoya et al., 2022).

Design of Experiments (DoE) is a systematic statistical framework used to plan, conduct, and analyzed controlled trials to evaluate the influence of multiple independent variables on a process. Within the DoE framework, Response surface methodology (RSM) represents a collection of statistical and mathematical approach used to model the relationship between multiple input variables and output responses and a powerful tool for process optimization (Myers et al., 2016). Therefore, it is frequently applied in chemical and biochemical processes, as it efficiently identifies key factors, their interactions, and optimal conditions with fewer experiments. Among several designs, Box-Behnken Design (BBD) and Central Composite Designs (CCD) are commonly used for RSM to fit quadratic polynomial equations (Czyrski and Jarzębski, 2020) and optimize process variables. BBD utilizes a three levels system for each factor and requires therefore fewer experimental runs than CCD as the number of factors increases. BBD is designed to evaluate factors within a strict range, avoiding the simultaneous combination of all extreme factor levels (Oza et al., 2022). In contrast, CCD is recognized for its robustness, especially for missing or limited data. By incorporating axial points that extend the design to five levels per factors, CCD allows for a more detailed exploration of the response surface (Ngan et al., 2014; Oza et al., 2022).

Several technologies have been investigated for producing pulp from *Miscanthus* × *giganteus* and/or *Miscanthus sinesis* including Kraft, Organosolv, and alkaline processes (Iglesias et al., 1996; Thykesson et al., 1998; Danielewicz et al., 2015; Bergs et al., 2021). While most previous studies have primarily reported pulp yield and Kappa number, focusing directly on end-product properties such as paper strength, few have examined the influence of wide range of processing conditions on the three major chemical components of the pulp, particularly for *Miscanthus* species (Muniz Kubota et al., 2018).

This study aims to increase our knowledge on the systematic interaction between processing parameters and the resulting chemical composition of the fiber using RSM, providing deeper insight into the alkaline-ethanol fractionation of *Miscanthus* × *giganteus*. The effects of temperature, cooking time, alkali concentration and ethanol concentration are examined with respect to pulp yield, chemical composition, and dissolved xylan in black liquor. Two experimental designs, representing low and high severity conditions, were conducted to evaluate the impact of processing variables across a broad range. Statistical analysis was then used to assess individual and interactive effects and to optimize the process under both severity levels. Finally, pulps obtained under optimal conditions were characterized morphologically to further elucidate fiber structure.

10.3389/fceng.2026.1791044

TABLE 1 Fractionation conditions on low severity (Design A) and on high severity (Design B).

Conditions	Design A	Design B
Cooking temperature (T)	80 °C ≤ T ≤ 140 °C	140 °C ≤ T ≤ 200 °C
Cooking times (t)	60 min ≤ t ≤ 160 min	110 min
Alkali concentration (NaOH %odw)	4 % ≤ NaOH ≤ 16 %	16 % ≤ NaOH ≤ 24 %
Ethanol concentration (EtOH %v/v)	0 % ≤ EtOH ≤ 60 %	30%

2 Materials and methods

2.1 Raw materials

Miscanthus × *giganteus* was harvested in April-May 2023 at the Klein-Altendorf campus, University of Bonn, Germany. The biomass was obtained as already dried material and subsequently stored in containers at room temperature. Prior to experimentation, the moisture content of the dried biomass was determined to be 8.3%. The feedstock was milled with a cutting mill (SM 200 Retsch, Haan, Germany) with a 1 mm sieve. NaOH (>99% purity), Ethanol

TABLE 2 Experimental design data for the low severity alkali-ethanol fractionation of *Miscanthus* × *giganteus* (Design A).

Run	Coded variable				Decoded variable			
	X_T	X_t	X_{NaOH}	X_{EtOH}	T (°C)	t (min)	NaOH (%odw)	EtOH (%v/v)
1	0	0	0	0	110	110	10	30
2	0	1	1	0	110	160	16	30
3	0	1	0	1	110	160	10	60
4	1	1	0	0	140	160	10	30
5	−1	0	0	−1	80	110	10	0
6	0	0	−1	1	110	110	4	60
7	0	0	−1	−1	110	110	4	0
8	0	1	−1	0	110	160	4	30
9	0	0	1	−1	110	110	16	0
10	0	0	0	0	110	110	10	30
11	0	0	0	0	110	110	10	30
12	−1	1	0	0	80	160	10	30
13	0	0	0	0	110	110	10	30
14	0	−1	−1	0	110	60	4	30
15	−1	0	−1	0	80	110	4	30
16	1	0	−1	0	140	110	4	30
17	−1	0	0	1	80	110	10	60
18	0	0	1	1	110	110	16	60
19	1	0	0	1	140	110	10	60
20	1	0	1	0	140	110	16	30
21	−1	−1	0	0	80	60	10	30
22	−1	0	1	0	80	110	16	30
23	0	0	0	0	110	110	10	30
24	0	−1	0	1	110	60	10	60
25	0	0	0	0	110	110	10	30
26	1	−1	0	0	140	60	10	30
27	0	−1	1	0	110	60	16	30
28	1	0	0	−1	140	110	10	0
29	0	1	0	−1	110	160	10	0
30	0	−1	0	−1	110	60	10	0

TABLE 3 Experimental design data for the high severity alkali-ethanol fractionation of *Miscanthus* × *giganteus* (Design B).

Run	Coded variable		Decoded variable	
	X_T	X_{NaOH}	T (°C)	NaOH (%odw)
1	0	0	110	10
2	0	1	110	16
3	0	0	110	10
4	1	0	140	10
5	−1	0	80	10
6	0	−1	110	4
7	0	−1	110	4
8	0	−1	110	4
9	0	1	110	16
10	0	0	110	10
11	0	0	110	10

TABLE 4 Chemical composition of *Miscanthus* × *giganteus* (*M. giganteus*) used in this work compared with reported literature values. Our results on the chemical composition are in good agreement with other studies.

Reference	This work	Brosse et al. (2009)	Frias and Feng (2013)	Lan et al. (2021)	Rivas et al. (2022)
Chemical component (%)	% dry basis				
Cellulose	42.3	37.7	42.8	36.1	65.8
Hemicellulose[a]	27.9	37.3		30.8	
Xylose	20.2	33.8	22	—	—
Lignin[b]	18.5	26.3	23.9	15.5	—
Acid-insoluble lignin (KL)	17.1	25.1	18.3	—	23.7
Acid-soluble lignin	1.4	1.2	5.6	—	—
Extractives[c]	6.6	—	7.7	—	—
Water extractives	4.7	—	3.5	—	—
Ethanol extractives	1.9	—	4.2	7.7	—
Ash	2.1	—	—	4.1	5.7
Acetic acid	2.1	—	3	—	—

[a]Hemicellulose is the sum of xylose, arabinose, mannose and galactose.
[b]Lignin is the sum of acid-insoluble lignin (Klason-lignin) and acid-soluble lignin.
[c]Extractives are the sum of water extractives and ethanol extractives.

(>98% purity), and standards for carbohydrates (arabinose, galactose, glucose, xylose, and mannose) acetic acid were purchased from Sigma-Aldrich (Germany).

2.2 Alkali-ethanol fractionation

All fractionation experiments for the DOE were carried out in a 25 mL stainless steel mini-scale autoclave digester (Tinyclave, Büchiglasuster, Switzerland) in heating blocks on stirring heating plates set to a constant speed of 1500 rpm. Each digester was loaded with 2 g of raw material (oven dry (o.d) basis) and an alkali-ethanol aqueous solution with a solid-to-liquid ratio of 1:10. The experiments were carried out under various conditions, including temperature (T), cooking time (t), alkali (NaOH) concentration (% o.d.weight), and ethanol concentration (%v/v in water), as shown in Table 1. The range of process variables was selected as low severity (Design A) and high severity (Design B), as described below. After the cooking time elapsed, the reactor was cooled in an ice bath, and the solid fraction was vacuum filtered. The separated solid was submerged in water at 40 °C, with the washing volume corresponding to twice the solvent volume used in the reaction. The liquid fraction from the initial separation (black liquor) and

10.3389/fceng.2026.1791044

TABLE 5 Experimental result data for the low severity alkali-ethanol fractionation (Design A).

Run	Dependent variables							
	Y (%)	C (%)	X (%)	L (%)	X_{BL} (mg)	CR (%)	XR (%)	LR (%)
1	70.28	57.13	25.18	8.06	123.10	94.99	87.56	69.41
2	62.66	59.70	25.74	5.75	124.45	88.49	79.81	80.54
3	66.62	57.64	27.02	5.35	36.78	90.85	89.06	80.75
4	64.92	57.41	25.44	6.44	163.35	88.17	81.72	77.44
5	75.76	53.27	23.53	13.42	98.27	95.47	88.20	45.08
6	83.26	49.73	22.32	16.40	21.43	97.95	91.97	26.26
7	86.01	48.19	21.84	19.54	27.79	98.06	92.92	9.23
8	82.90	49.27	21.89	18.36	42.72	96.63	89.77	17.80
9	63.25	62.40	23.54	5.60	150.00	93.36	73.67	80.89
10	67.97	58.38	25.36	7.20	123.67	93.87	85.30	73.56
11	67.65	58.10	24.79	7.54	100.33	92.98	82.98	72.46
12	73.51	55.61	24.91	9.57	91.83	96.72	90.60	62.01
13	67.84	57.50	24.77	8.11	93.32	92.29	83.15	70.29
14	83.24	49.47	23.78	16.37	65.08	97.43	97.94	26.42
15	86.47	49.74	22.60	17.43	37.90	101.76	96.70	18.59
16	81.43	50.65	23.42	15.23	64.50	97.58	94.33	33.02
17	77.88	53.56	24.60	11.30	35.33	98.68	94.80	52.46
18	66.55	57.68	25.90	6.78	23.83	90.81	85.27	75.62
19	65.30	56.83	26.25	6.52	32.52	87.79	84.80	77.01
20	62.20	62.77	25.40	3.71	163.97	92.36	78.18	87.54
21	74.91	53.11	24.31	12.39	86.21	94.12	90.10	49.89
22	68.84	56.15	23.60	10.43	164.66	91.45	80.39	61.24
23	68.40	56.68	24.59	8.21	90.45	91.71	83.23	69.67
24	73.54	53.04	24.28	11.00	23.82	92.27	88.34	56.32
25	68.87	56.48	25.29	7.92	113.06	92.01	86.17	70.56
26	66.28	58.42	25.48	5.99	118.12	91.60	83.57	78.56
27	65.60	58.29	24.02	7.89	155.25	90.47	77.97	72.04
28	63.37	59.20	23.71	7.42	125.63	91.05	76.25	73.94
29	67.59	57.52	24.45	8.14	108.31	91.97	81.78	70.30
30	70.52	56.52	23.74	9.87	100.43	94.30	82.83	62.42

washing steps (wash) were collected and stored at 5 °C until further analysis. The pulps were then washed an additional time with approximately 300 mL of water, oven-dried at 65 °C until it reached a constant weight, and pulp yield was determined gravimetrically by dividing its weight by that of the initial raw material.

Fractionation at the identified optima was conducted in a 300 mL stainless steel autoclave digester equipped with a stirring motor (Miniclave drive, Büchiglasuster, Switzerland), using 20 g of raw material (oven dry basis) at a solid-to-liquid ratio of 1:10. The reactor was heated to the optimum temperature with a heating mantel (Winkler AG, Germany) and maintained for the optimum cooking time. After completion, the reactor was cooled in an ice bath. Separation of solid and liquid fraction followed the same procedure as for the 25 mL reactor.

TABLE 6 Model equations in terms of coded factors and corresponding statistical parameter from ANOVA (Design A).

Dependent variable	Equation	Regression parameter	Model (p)	LoF (F)	Outlier run
Y	$Y = 68.55 - 4.49X_T - 1.32X_t - 9.52X_{NaOH} + 0.5546X_{EtOH} + 1.51X_{NaOH}X_{EtOH} + 1.15X_T^2 + 5.10X_{NaOH}^2 + 0.9995X_{EtOH}^2$	$R^2 = 0.9764$ Adj. $R^2 = 0.9544$	<0.0001	3.4400	-
C	$C = 57.38 + 1.99X_T - 0.6917X_t + 5X_{NaOH} - 0.7183X_{EtOH} - 0.8755X_TX_t + 1.43X_TX_{NaOH} + 0.9X_t$ $X_{EtOH} - 1.57X_{NaOH}X_{EtOH} - 0.6062X_T^2 - 0.6962X_t^2 - 2.19X_{NaOH}^2 - 0.7488X_{EtOH}^2$	$R^2 = 0.9764$ Adj. $R^2 = 0.9544$	<0.0001	1.2100	-
X	$X = 25.03 + 0.5118X_T + 0.3206X_t + 1.03X_{NaOH} + 0.7969X_{EtOH} + 0.9041X_tX_{NaOH} + 0.5056X_tX_{EtOH} + 0.4665X_{NaOH}X_{EtOH} - 1.24X_{NaOH}^2 - 0.3508X_{EtOH}^2$	$R^2 = 0.9764$ Adj. $R^2 = 0.9544$	<0.0001	2.7200	-
L	$L = 8.28 - 2.44X_T - 0.8252X_t - 5.26X_{NaOH} - 0.5331X_{EtOH} - 1.13X_TX_{NaOH} - 1.03X_tX_{NaOH} - 0.9795X_tX_{EtOH} + 1.08X_{NaOH}X_{EtOH} + 3.45X_{NaOH}^2 + 0.6848X_{EtOH}^2$	$R^2 = 0.9764$ Adj. $R^2 = 0.9544$	<0.0001	8.5800	-
X_{BL}	$X_{BL} = 106.78 + 12.82X_T + 43.56X_{NaOH} - 36.39X_{EtOH} - 29.95X_{NaOH}X_{EtOH} - 41.43X_{EtOH}^2$	$R^2 = 0.9764$ Adj. $R^2 = 0.9544$	<0.0001	1.7800	-
CR	$CR = 93.23 - 2.93X_T - 0.6133X_t - 3.08X_{NaOH} - 0.4883X_{EtOH} - 1.51X_TX_t + 2.66X_TX_{NaOH} - 1.62X_TX_{EtOH} - 0.9145X_t^2 + 1.31X_{NaOH}^2$	$R^2 = 0.9764$ Adj. $R^2 = 0.9544$	<0.0001	0.9081	16
XR	$XR = 85.70 - 4.18X_T - 0.6663X_t - 6.68X_{NaOH} + 3.22X_{EtOH} + 2.10X_TX_{NaOH} + 2.50X_tX_{NaOH} + 3.14X_{NaOH}X_{EtOH}$	$R^2 = 0.9764$ Adj. $R^2 = 0.9544$	<0.0001	0.8016	16
LR	$LR = 70.42 + 11.52X_T + 3.60X_t + 27.21X_{NaOH} + 2.21X_{EtOH} + 4.28X_tX_{NaOH} + 4.14X_tX_{EtOH} - 5.57X_{NaOH}X_{EtOH} - 3.06X_T^2 - 19.01X_{NaOH}^2 - 3.87X_{EtOH}^2$	$R^2 = 0.9764$ Adj. $R^2 = 0.9544$	<0.0001	9.5500	-

10.3389/fceng.2026.1791044

10.3389/fceng.2026.1791044

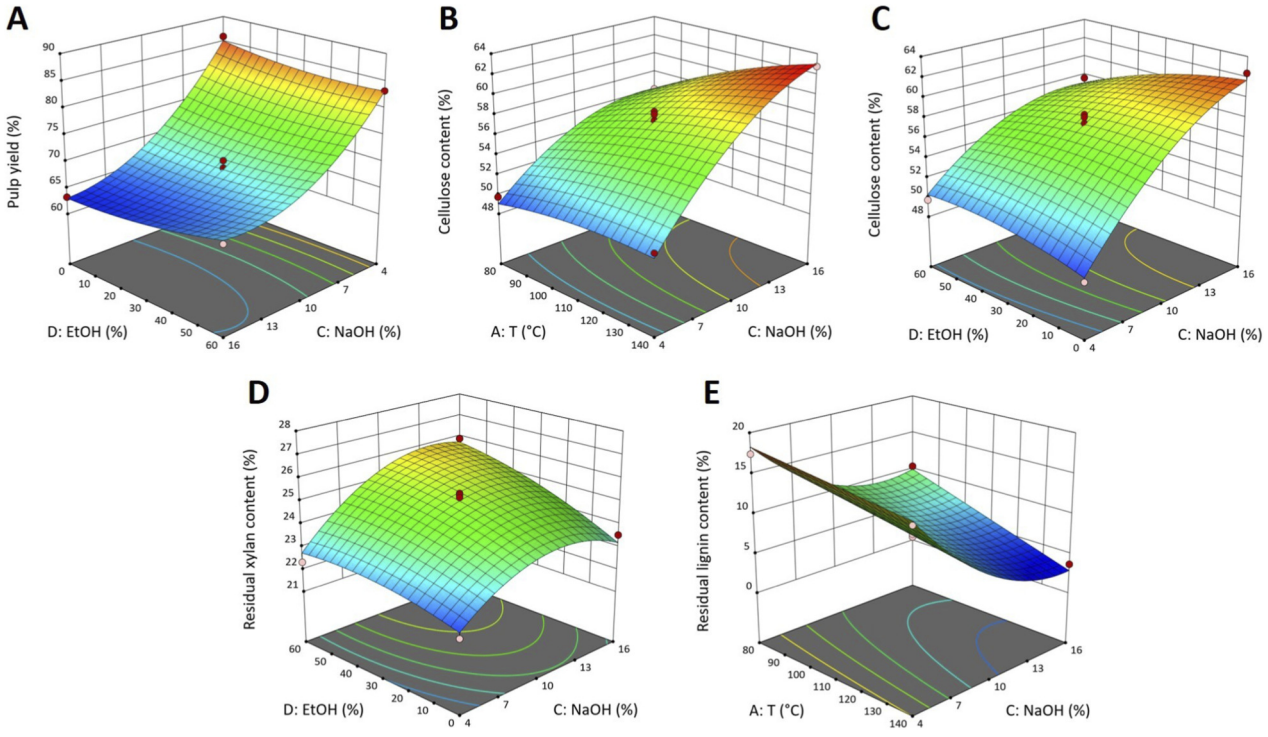

FIGURE 1
Response surface plots showing interaction effect between process variables on pulp properties at fixed condition of the other two factors (Design A): **(A)** NaOH and EtOH interaction effect on pulp yield (Y). **(B)** T and NaOH interaction effect on cellulose content (C). **(C)** NaOH and EtOH interaction effect on cellulose content (C). **(D)** NaOH and EtOH interaction effect on residual xylan content (X). **(E)** T and NaOH interaction effect on residual lignin content (L). Experimental data is marked with red circles.

2.3 Raw material and product characterization

The raw biomass, produced pulp and black liquor were characterized regarding product quality and process performance by determining the chemical composition. The structural carbohydrates and lignin of the raw material and obtained pulps were measured according to the National Renewable Energy Laboratory (NREL) protocol (Sluiter et al., 2012). Briefly, 300 mg of the material was hydrolyzed in a 72% H_2SO_4 solution for 60 min in a water bath set at 30 °C, and then hydrolysates were diluted to a 4% H_2SO_4 solution and autoclaved at 121 °C for 60 min. Sugar Recovery Standards (SRS), consisting of known concentrations of relevant monosaccharides, were processed through the autoclave stage in parallel to calculate correction factors for sugar degradation. The autoclaved solutions were vacuum filtered using pre-weighted filtering crucibles to gravimetrically determine the acid-insoluble lignin (AIL). The liquor obtained after filtering was used to measure the acid-soluble lignin by measuring the solution's absorbance at 205 nm using a UV-Vis spectrometer. Liquor aliquots were used to quantify the sugar content and acetyl content by high-performance liquid chromatography (HPLC) using a carbohydrate $Pb2^+$ and an organic acid column, respectively (CS Chromatographie, Germany). Quantification was performed using external calibration standards for each analyzed component. For sugar analysis, the liquor was neutralized to pH 6–7 with $CaCO_3$, filtered through a 0.2 µm syringe filter, and injected into the HPLC. Separation was performed using water as eluent at 0.6 mL/min and 80 °C with refractive index detection. For acetyl content analysis, the liquor was filtered without neutralization and analyzed by HPLC under the same detection method, using 0.005 M sulfuric acid as eluent at 0.6 mL/min and 55 °C. The extractives and ash content were determined by NREL protocol (Sluiter et al., 2005a; 2005b). The liquid fraction (black liquor and wash) was characterized for total dissolved sugars according to the NREL protocol (Sluiter et al., 2006). Both liquid fractions were concentrated by evaporation if ethanol was present. Then, 3 mL of the concentrated liquor was diluted in water, autoclaved with a 4% H_2SO_4 solution at 121 °C for 60 min, and processed in the same manner as the solid fractions described above. The amount of dissolved xylose in both liquors was determined by multiplying the concentration measured *via* HPLC by the total cooking liquor volume and the dilution factor. The total dissolved xylan amount was then expressed as the total mass (mg) recovered from the combined liquid fractions. Cellulose was estimated as glucan (glucose × 0.9), and hemicelluloses were estimated by adding the results of xylan (xylose × 0.88), mannan (mannose × 0.9), arabinan (arabinose × 0.88), and galactan (galactose × 0.9) according to the NREL protocol (Sluiter et al., 2012).

The cellulose, xylan retention and lignin removal (*i*R) was calculated as:

$$iR = \begin{cases} \dfrac{C_{i,pulp} \cdot m_{pulp}}{C_{i,raw} \cdot m_{raw}} \times 100, i = \text{C (Cellulose) or X (Xylan)} \\ \left(1 - \dfrac{C_{i,pulp} \cdot m_{pulp}}{C_{i,raw} \cdot m_{raw}}\right) \times 100, i = \text{L (Lignin)} \end{cases} \quad (1)$$

10.3389/fceng.2026.1791044

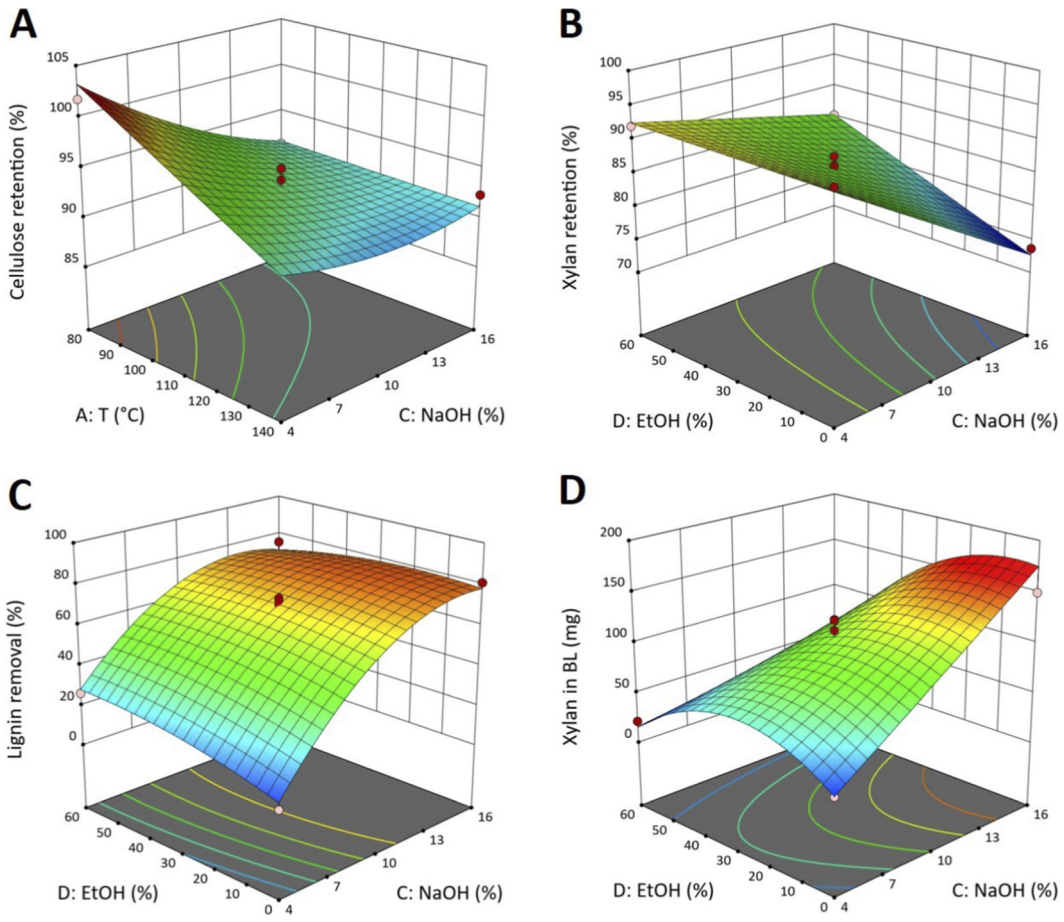

FIGURE 2
Response surface plots showing interaction effect between process variables on pulp properties at fixed condition of the other two factors (Design A): **(A)** T and NaOH interaction effect on cellulose retention (CR).; NaOH and EtOH interaction effect on **(B)** xylan retention (XR); **(C)** lignin removal (LR). **(D)** xylan in black liquor (X_{BL}). Experimental data is marked with red circles.

where

$C_{i,raw}$: Mass fraction of component i in raw biomass (% dry basis)

$C_{i,pulp}$: Mass fraction of component i in pulp (% dry basis)

$m_{raw\ or\ pulp}$: Oven-dry mass of raw biomass or pulp (g)

The subscript i identifies the component (e.g., L for lignin).

In this context, retention quantifies the percentage of a desired component preserved in the pulp relative to the initial biomass, while removal quantifies the percentage of an undesired component extracted from it.

The fiber morphology of the achieved pulps at optima was measured using an L&W Fiber Tester Plus (ABB, Switzerland). To prepare the sample, 300 mg of pulp was submerged in approximately 300 mL of water containing 50 µL of the non-ionic surfactant (Triton-X-100). The sample was then thoroughly disintegrated using a motor for 10 min. For measurement, 100 mL aliquots of this solution were used for each reading, and all measurements were performed in triplicate. The length-weighted average of length, width of fiber on the pulp, fines, fibril perimeter, and average kink index are reported in this work.

2.4 Experimental design

Response surface methodology (RSM) was used to investigate the effects of process variables on the responses, allowing the optimization of the fractionation process. The alkaline-ethanol fractionation study comprised two experimental designs. Design A targeted a low severity domain to identify the most significant process variables affecting pulp quality. Subsequently, Design B explored a high severity domain, constrained to the two dominant factors identified in Design A. The experimental ranges for both regimes were defined based on established literature for the alkaline and alkali-ethanol fractionation of non-wood biomass.

For Design A, the parameters were selected to reflect the mild conditions necessary for fiber liberation while minimizing carbohydrate degradation. NaOH concentration range was determined based on the findings that up to 15% of the chemical represents the critical amount necessary for the efficient delignification of Arundo donax L., as demonstrated by changes in pulp yield and residual lignin content (Shatalov and Pereira, 2004). Temperature boundaries were determined by delignification

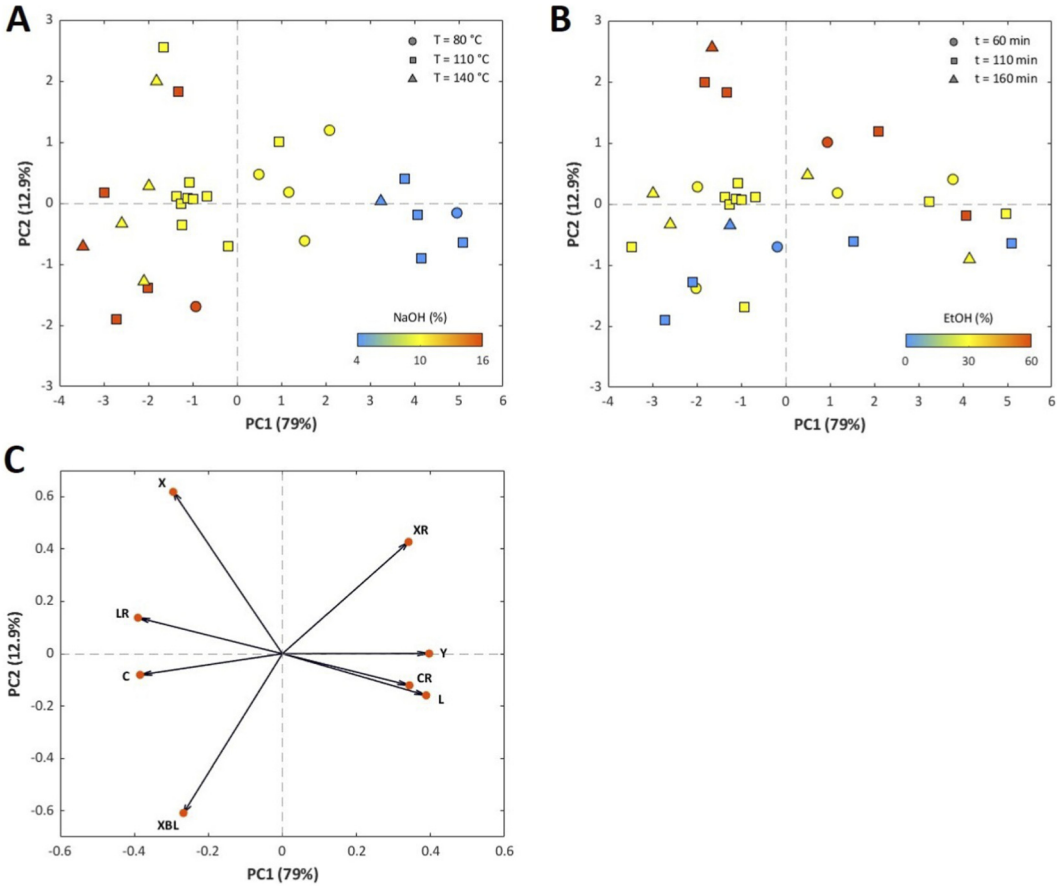

FIGURE 3
Scores plot of PCA using responses in Design A; **(A)** Point shape: temperature (T), color map: NaOH concentration **(B)** Point shape: time (t), color map: ethanol concentration **(C)** Loads plot of PCA for responses in Design A.

kinetics. The process is primarily diffusion-controlled at temperatures up to 140 °C (Biermann, 1993; Sahin and Young, 2008), while previous studies have demonstrated the efficient delignification of *Miscanthus* starting above 80 °C (Iglesias et al., 1996). Furthermore, the reaction time window was determined to capture of rapid phase of solubilization, which typically occurs within the first hour of cooking for *Miscanthus*, as shown by Iglesias et al. This range also allows the observation of the transition into the bulk delignification phase, aligning with the literatures (Shatalov and Pereira, 2004; Carvalho et al., 2014). The ethanol concentration range was selected to evaluate the transition from alkaline fractionation to ethanol-reinforced system (Carvalho et al., 2014; Dagnino et al., 2017; Berhanu et al., 2018). Design B was engineered to explore the upper intensity limits of fractionation process. The maximum cooking temperature was limited to 200 °C to avoid the severe fiber degradation and hemicellulose loss typical of extreme thermal treatments (Sahin and Young, 2008; Aklilu, 2020). The upper limit of NaOH concentration was set at 24%, aligning with the typical severe alkaline fractionation conditions established in literatures (Shakhes et al., 2011; Lemma et al., 2023). This sequential RSM framework ensured the validity of the response models across a broad range of process severities.

The process was evaluated using the following directly measured responses: pulp yield (Y), the cellulose content (C), the residual xylan content (X), and the residual lignin content (L) in the solid pulp, and the concentration of dissolved xylan in the black liquor (X_{BL}). From this primary data, key performance indicators were calculated according to Equation 1, including cellulose retention (CR), xylan retention (XR), and lignin removal (LR).

The experimental data for each response was modeled by fitting a second-order polynomial equation (Equation 2) using multiple regression analysis and the least squares method.

$$Y = \beta_0 + \sum_{i=1}^{k} \beta_{ii} x_i^2 + \sum_{i=1}^{k-1} \sum_{j=i+1}^{k} \beta_{ij} x_i x_j, Y \in [\mathrm{Y}, \mathrm{C}, \mathrm{X} \ldots] \quad (2)$$

Where Y is the predicted responses (i.e., pulp yield or cellulose content or *etc.*), k is the number of independent variables, β_0, β_i, β_{ii}, and β_{ij} are the regressions coefficients for intercept, linear, quadratic, and interaction terms, respectively and x_i and x_j are the coded values of the independent variables.

Design A- Fractionation at low severity: To address the challenges posed by the large parameter space, a sequential Response Surface Methodology (RSM) was adopted. Initially, a Box-Behnken Design (BBD) was used to formulate model

10.3389/fceng.2026.1791044

TABLE 7 Experimental result data for the high severity alkali-ethanol fractionation (Design B).

Run	Dependent variables							
	Y (%)	C (%)	X (%)	L (%)	X_{BL} (mg)	CR (%)	XR (%)	LR (%)
1	53.33	66.55	22.83	3.74	184.10	83.96	54.12	89.23
2	53.99	66.94	23.19	3.07	182.47	85.50	55.95	91.04
3	54.87	66.22	23.76	3.45	182.04	86.00	57.62	89.78
4	55.32	66.21	23.56	3.50	186.95	86.65	57.83	89.55
5	55.38	65.91	23.85	3.45	183.81	86.35	58.80	89.67
6	58.54	63.16	25.28	4.18	175.29	87.47	66.07	86.79
7	59.50	62.53	25.57	4.19	162.48	88.02	68.09	86.53
8	54.67	66.01	23.10	4.01	148.69	85.38	56.34	88.15
9	57.80	64.61	23.78	3.96	155.59	88.35	62.12	87.63
10	55.84	64.63	23.61	4.14	182.72	85.38	60.31	87.52
11	49.97	69.00	21.34	3.16	180.46	81.57	47.49	91.46

equations for each response and screen four operating variables: temperature, time, NaOH concentration, and ethanol concentration (Table 1). The BBD was chosen for its high efficiency in managing multiple factors, providing an overview of parameter interactions within the low severity regime. This design is particularly effective for evaluating factors within a restricted range while avoiding combinations of extreme process conditions. The variable range was selected to represent mild conditions. BBD utilized three levels for each factor, coded as −1, 0, +1, representing low, medium and high values of the experimental factors, respectively. A total of 30 runs were performed including 16 runs at the edge points (±1 for two factors and 0 for the other two), 8 runs at the midpoint of the edges (0 for two factors, ±1 for the other two), and 6 center points (all factors at 0), as shown in Table 2.

Design B- Fractionation at high severity: After analyzing the data from Design A, the significant factors were determined to be temperature and NaOH concentration. To efficiently explore these key factors at higher intensities, the design space was narrowed, and a Central-Composite Design (CCD) was employed for Design B. This split-design approach allowed for a more detailed characterization of the high-severity regime while reducing the overall experimental burden. During this phase, time and ethanol concentration were held at the midpoint of the edges from Design A. CCD for Design B was selected for its robustness and ability to model the response surface curvature with higher detail by incorporating axial points, extending the factors to five levels (coded as ± α, ± 1, 0). A total of 11 runs were performed for Design B, including 4 factorial points, 4 axial points and 3 center points, as shown in Table 3.

The model coefficients were obtained using Design-Expert version 13 software (Stat-Ease Inc., Minneapolis, United States of America). Analysis of variance (ANOVA) was applied to identify the significance of individual and interaction effects of each variable. The coefficient of determination R^2, adjusted R^2 and lack of fit from ANOVA were used to determine the statistical significance of the developed model. Numerical optimization based on the desirability function was then carried out to achieve the desired goals of each response. The optimum condition obtained by RSM was then confirmed experimentally.

Principal component analysis (PCA) was performed on the data from both experimental designs to visualize the primary trends and correlations among the measured responses. Prior to analysis, all responses variables were auto-scaled (mean-centered and scaled to unit variance) to ensure equal contribution to the model. The analysis was performed in MATLAB (R2023b, The MathWorks, Inc.).

3 Results and discussion

A set of response variables was selected for analysis to understand the interactions between process parameters and their effects on product quality and process efficiency. These variables are grouped into three key areas: final pulp quality, fractionation efficiency, and sugar degradation.

Pulp quality was defined by the chemical composition of the final solid product, specifically the cellulose content and the amounts of residual xylan and residual lignin. These values provide the fundamental chemical profile of the resulting pulp's purity and composition. In contrast, fractionation efficiency, a dynamic indicator of process performance, was evaluated based on cellulose and xylan retention and lignin removal relative to the raw biomass composition. Analyzing both composition and efficiency is crucial, as a high cellulose content in the pulp could be misleading if the overall cellulose retention is low due to significant mass loss. To evaluate the hemicellulose valorization potential, polysaccharide degradation was monitored by measuring the xylan concentration in the black liquor. Minimizing this degradation is essential for preserving the dissolved sugars as a viable feedstock for value-added products. Since *Miscanthus* has up

TABLE 8 Model equations in terms of coded factors and corresponding statistical parameter from ANOVA (Design B).

Dependent variable	Equation	Regression parameter	Model (p)	LoF (F)	Outlier run
Y	$Y = 55.38 - 2.65X_T - 2.03X_{NaOH}$	$R^2 = 0.9663$ Adj. $R^2 = 0.9578$	<0.0001	4.60	-
C	$C = 65.98 + 1.87X_T + 1.24X_{NaOH} - 0.6637X_T^2$	$R^2 = 0.9742$ Adj. $R^2 = 0.9485$	0.0006	8.18	-
X	$X = 23.62 - 1.20X_T - 0.7181X_{NaOH}$	$R^2 = 0.9048$ Adj. $R^2 = 0.8810$	<0.0001	9.07	-
L	$L = 3.45 - 0.2657X_T - 0.2349X_{NaOH} - 0.1988X_TX_{NaOH} + 0.5243X_T^2 - 0.1108X_{NaOH}^2$	$R^2 = 0.9932$ Adj. $R^2 = 0.9848$	<0.0001	6.65	9
X_{BL}	$X_{BL} = 182.44 + 13.15X_{NaOH} - 13.70X_{NaOH}^2$	$R^2 = 0.9316$ Adj. $R^2 = 0.8633$	<0.0062	5.69	-
CR	$CR = 86.57 - 1.66X_T - 1.55X_{NaOH} - 1.27X_T^2$	$R^2 = 0.9667$ Adj. $R^2 = 0.9334$	0.0011	3.28	-
XR	$XR = 58.61 - 6.09X_T - 3.80X_{NaOH}$	$R^2 = 0.9702$ Adj. $R^2 = 0.9627$	<0.0001	3.65	-
LR	$LR = 89.65 + 1.33X_T + 1.06X_{NaOH} + 0.5798X_TX_{NaOH} - 1.62X_T^2 + 0.3748X_{NaOH}^2$	$R^2 = 0.9973$ Adj. $R^2 = 0.9939$	<0.0001	1.77	9

to 30% of hemicellulose (Da Costa et al., 2017; Schäfer et al., 2019), the xylan concentration in the liquor provides insight into the degradation pathways, such as alkaline hydrolysis and end-group peeling reactions, during fractionation (Sjöström, 1991).

3.1 Characterization of raw material

The chemical composition analysis of *Miscanthus* × *giganteus* used in this study is presented in Table 4, alongside four representative datasets from the literature. Our results on the chemical composition are in good agreement with other studies. Our measurements show typical amounts of cellulose (42.3%) and hemicellulose (27.9%), but a comparatively lower lignin content (18.5%) than reported data.

3.2 Fractionation at low severity (design A)

3.2.1 RSM-ANOVA

Table 5 shows the dependent variables obtained from all experiments conducted in Design A, including the directly measured responses: pulp yield (Y), cellulose content (C), residual xylan content (X), residual lignin content (L) in the solid pulp, concentration of dissolved xylan in the black liquor (X_{BL}), and the calculated performance indicators: cellulose retention (CR), xylan retention (XR), and lignin removal (LR). The statistical significance of the linear, interaction, and quadratic effects of all the variables was predicted by ANOVA. Table 6 summarizes the model equations in terms of the coded values of the variables for each response and the regression and model parameters, including the p-value of the model, the F-value of the lack of fit (LoF), and the outlier run. For all responses in Design A, the overall model p-values were lower than 0.05, indicating statistically significant regression models. The F-value of LoF, defined as the ratio of the mean square for lack of fit to the pure error, were insignificant, demonstrating that the fitted models adequately describe the experimental data within the investigated design space (Montgomery, 2017). The outlier runs, identified by their significant deviation in the 'Predicted vs. Actual' and Cook's Distance diagnostic plots (high residual error), were excluded to minimize noise and improve the regression model statistics. The model equations include only statistically significant linear, quadratic, and interaction terms, refined through backward elimination (using an alpha-to-exit of 0.1). This systematic removal of insignificant terms slightly changes the coefficients compared to those in the complete equations, which include both significant and insignificant terms (see Supplementary Equations S1–S8). The terms in the equations can be positive or negative, reflecting the direction of their influence on the response variables. Temperature, time and NaOH concentration influence the responses in the same direction. These three variables act synergistically by collectively determining the intensity of the fractionation process, whereby higher intensity enhances lignin removal and carbohydrate dissolution but reduces pulp yield and carbohydrate retention. Ethanol concentration acts differently from the other factors–its increase enhances pulp yield, residual xylan content, xylan retention and lignin removal, but suppresses cellulose and residual lignin content, and cellulose retention.

A complete ANOVA for all terms is shown in Supplementary Table S1. One can determine the significance of each factor by calculating the p-value. A p-value for a term less than 0.05 indicates that the model term is significant. The results indicate that NaOH concentration and temperature are significant factors affecting all responses, while time and ethanol concentration only affect selected responses. Time is a significant factor for all responses except carbohydrate retention and xylan dissolution. Ethanol concentration mainly affects cellulose content and the xylan-

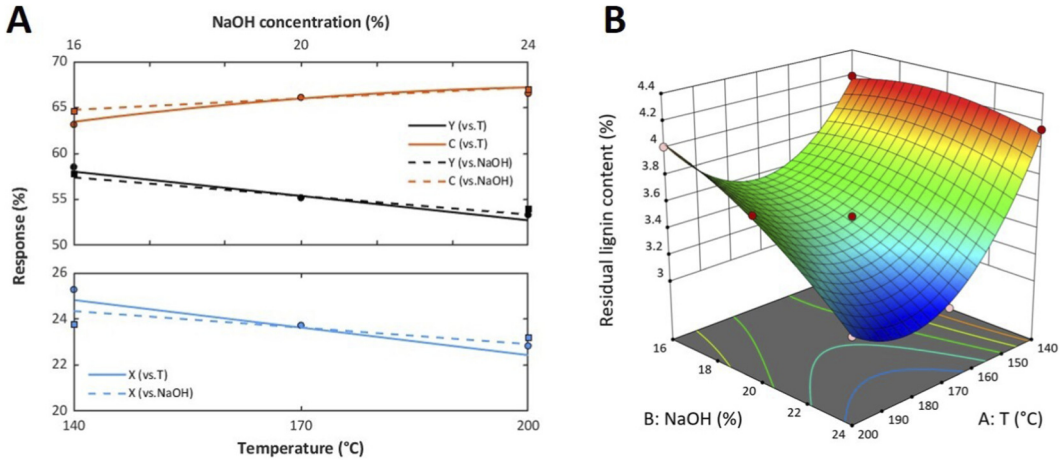

FIGURE 4
Linear response plot at fixed condition of the other factor (Design B): **(A)** T (full line) and NaOH (dotted line) effect on pulp yield (Y), cellulose content (C), residual xylan content (X). Experimental data is marked with circles (vs. T) and squares (vs. NaOH) **(B)** response surface plot of T and NaOH interaction effect on residual lignin content (L). Experimental data is marked with red circles.

related parameters. The each statistically significant response for Design A described below will be assessed using the p-values reported in Supplementary Table S1.

3.2.2 Response surface

Based on ANOVA, the significant factors affecting each response of Design A were visualized through three-dimensional response surface plots (Figures 1, 2). In these plots, the two factors were fixed at the midpoint values and the other two factors varied within their experimental range.

3.2.2.1 Pulp yield and chemical composition

For Design A, the pulp yields obtained in the experiment were in the range of 62.2%–86.47% (Table 5). As shown in Supplementary Table S1, pulp yield was significantly affected by the temperature, NaOH concentration, and time. The interactive effect of NaOH and ethanol concentration is considerable ($p = 0.0751$). The response surface plot (Figure 1A) shows that pulp yield decreases sharply with increasing NaOH concentration. Ethanol concentration exhibits only a minor interactive effect, shifting from a slight negative to a slight positive influence with increasing NaOH.

Cellulose content ranged from 48.19% to 62.77%. All factors and most of their interactions, except the interaction between temperature-EtOH and time-NaOH, significantly affected the cellulose content of the pulp. As shown in Figure 1B, the synergistic effect of temperature and NaOH is apparent, with the highest cellulose content being obtained at the maximum process severity. This indicates that increased concentration of hydroxyl ions and temperature cause a substantial loss of hemicelluloses and the dissolution of lignin into the pulping liquor, thereby enhancing the cellulose percentages in the pulp (Mohamad and Jai, 2022). In contrast, increasing ethanol concentration at a high alkali concentration decreased the cellulose content of the pulp (Figure 1C), which can be explained by the increased residual xylan content displayed in Figure 1D.

Residual xylan content ranged from 21.83% to 27.02%, with all four factors as well as the interactions of time with NaOH and EtOH, being significant. The NaOH-EtOH interaction was also notable ($p = 0.0641$). The interactive effect of NaOH and EtOH exhibited opposite trends for cellulose and xylan: Ethanol promoted hemicellulose preservation, leading in higher xylan and slightly lower cellulose contents in the pulp. Shatalov et al. studied the influence of ethanol on pulp quality by ethanol-alkaline pulping of *Arundo donax* L. (Shatalov, 2002). They reported that xylan content of the pulp increased from 8.6% to 12.1% (% on o. d. reed), while glucan content decreased from 30.5% to 29.83% as ethanol concentrations rose from 20% to 60%, aligning with this study.

Residual lignin contents were in the range of 3.71%–19.54%. It was significantly affected by NaOH concentration, temperature, and time, while the effect of ethanol concentration was also considerable ($p = 0.0645$). In addition, interactions between NaOH concentration and the other three variables had significant impacts on lignin content. Complementary to the cellulose content changes shown by the interaction between NaOH concentration and temperature (Figure 1B), the lowest residual lignin content was obtained at the highest NaOH concentration and temperature (Figure 1E).

3.2.2.2 Fractionation efficiency

Cellulose and xylan retention after pulping refers to the extent to which carbohydrates from cellulose and hemicellulose are preserved in the pulp. This is crucial for optimizing pulp quality and enhancing the efficiency due to an increased pulping yield and positive effects on pulp beating and strength properties (Fardim and Durán, 2004).

Cellulose retention ranged from 87.79% to 101.76%. The value slightly over-100% in run 15 is attributed to cumulative analytical errors, including biomass heterogeneity and minor overestimation of pulp yield. Temperature and NaOH concentration as well as the interaction of temperature with the other variables significantly affected cellulose retention. Figure 2A illustrates the interactive

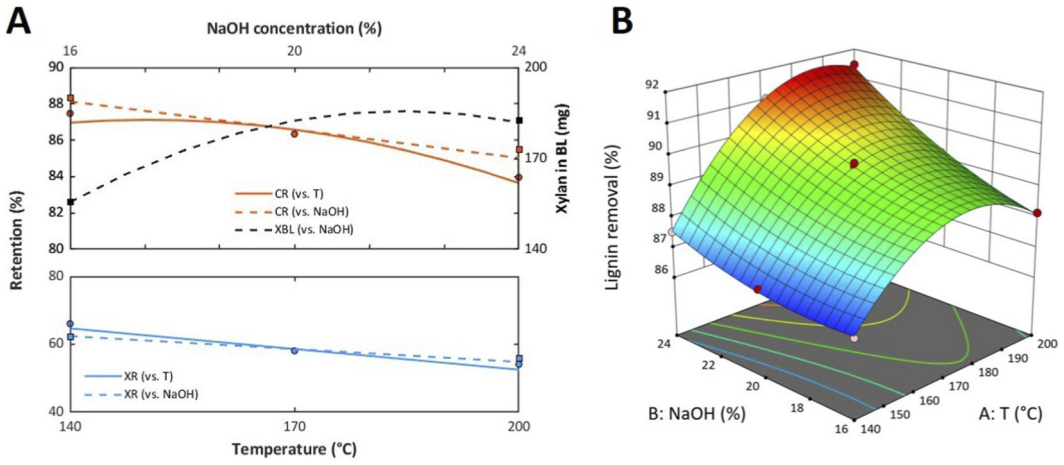

FIGURE 5
Linear and quadratic response plots at fixed condition of the other factor (Design B): **(A)** T (full line) and NaOH (dotted line) effect on cellulose retention (CR), xylan retention (XR), and xylan content in black liquor (X_{BL}) Experimental data is marked with circles (vs. T) and squares (vs. NaOH) **(B)** response surface plot of T and NaOH interaction effect on lignin removal (LR).

effect of temperature and NaOH concentration, demonstrating that cellulose retention decreases sharply as NaOH concentration and temperature increase.

Xylan retention ranged from 73.67% to 97.94%. Statistical analysis confirmed that the effect of temperature, NaOH concentration and ethanol concentration, alongside the interactions of NaOH concentration with temperature, time and ethanol concentration, were significant for xylan retention. Although time significantly affected the residual xylan content in the pulp ($p = 0.0310$), its actual contribution to xylan dissolution was relatively minor, as reflected by the comparable xylan content in black liquor ($p = 0.7719$). The synergistic interaction between temperature and NaOH concentration ($p = 0.0976$) suggests that these two factors influence hemicellulose removal together, confirming that these are the important factors governing the disruption of the biomass structure. Figure 2B clearly shows the interaction between ethanol and NaOH concentration on xylan retention. Zhang and Wu reported that, increasing the ethanol concentration from 40% to 80% during ethanol-assisted pretreatment of sugarcane bagasse significantly reduced xylan removal from 85.6% to 40.2% (Zhang and Wu, 2014). The presence of ethanol reduces hemicellulose solubility, thus preserving its integrity and mitigating hydrolysis reactions that facilitate hemicellulose degradation (Peng et al., 2019; He et al., 2020). This reduced xylan solubilization is linked to the lower delignification due to the lignin-hemicellulose linkages. A similar tendency was observed in this study: as the ethanol concentration increased, the xylan retention increased while the lignin removal slightly decreased, particularly at higher NaOH concentrations (Figure 2C).

Lignin removal varied substantially within Design A (9.23%–87.54%), reflecting the strong effects of temperature, NaOH concentration, and time, and the interaction between NaOH and EtOH concentration. Here ethanol concentration does not directly govern delignification, but its influence shifts with alkalinity, promoting lignin removal at low NaOH levels and suppressing it under more severe alkaline conditions.

The removed xylan amount from pulp varied from 21.43 to 164.66 mg. Temperature, NaOH and ethanol concentration and interaction between NaOH and ethanol significantly affected xylan dissolution. Temperature and NaOH are known to drive xylan degradation in aqueous alkaline systems *via* peeling reactions and alkaline hydrolysis (Sjöström, 1977). However, in our system at low severity, this degradation trend is not observed. While higher NaOH concentration and temperature clearly enhances the initial solubilization and removal of xylan from the biomass, the competing preservative role of ethanol (promoting retention) appears to be the dominant controlling factor overall. The response surface plot of NaOH and EtOH in Figure 2D presents the impact of the interaction between NaOH and ethanol concentration. NaOH concentration serves as the primary agent for xylan cleavage, while the presence of ethanol modulates the solubility of these fragments. At low NaOH concentration, the extent of xylan cleavage is inherently limited, making the presence of ethanol less impactful on overall dissolution of xylan. However, at high alkali charges, where the potential for xylan solubilization is maximized, the role of ethanol becomes critical. At high NaOH concentration, where extensive xylan cleavage occurs, a higher ethanol concentration greatly decreases the ability of black liquor to dissolve xylan. This reduced solvation ability results in less dissolved xylan being recovered in the liquid fraction, which corresponds to higher xylan retention in the pulp.

3.2.3 Multivariate analysis

A PCA was conducted using all response variables to summarize the overall relationships between the process parameters and the response variables, as well as the interrelations among the responses.

The first two principal components (PC1 and PC2) were selected, accounting for 79.0% and 12.9%, respectively. The

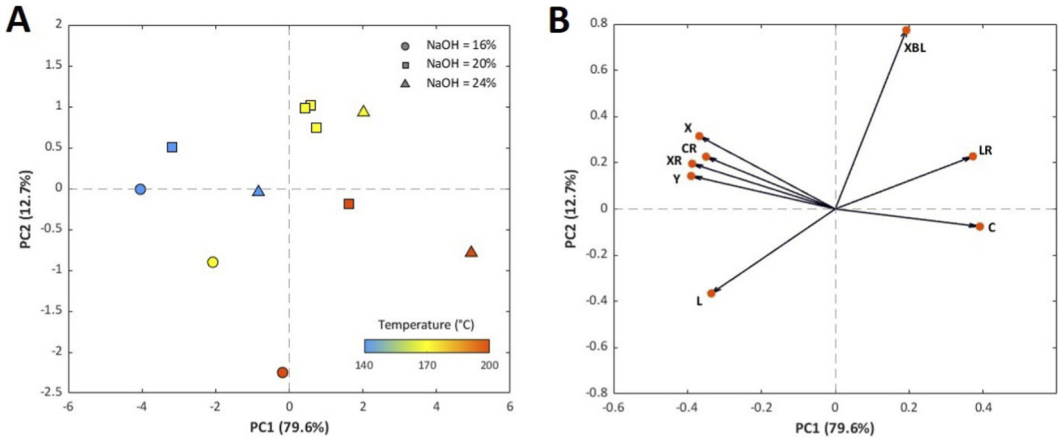

FIGURE 6
(A) Scores plot of PCA using responses in Design B. Point shape: NaOH concentration; color map: temperature (T) **(B)** Loads plot of PCA for responses in Design B.

score plot (Figure 3A) reveals that the experiments were primarily separated along the PC1 axis according to NaOH concentration, with temperature providing a secondary, reinforcing trend (color map: NaOH concentration; point shape: temperature). Increasing either NaOH or temperature leads to more negative PC1 scores, indicating that PC1 represents the overall intensity of the fractionation process. The loading plot (Figure 3C) corroborates this interpretation by showing that pulp yield (Y), cellulose retention (CR), residual lignin content in pulp (L) and xylan retention (XR) are associated with positive PC1 scores (lower process intensity in Design A), whereas cellulose content (C), lignin removal (LR), residual xylan content (X) and xylan content in black liquor (XBL) load negatively on PC1 (higher process intensity). Thus, a higher process intensity within the range of Design A enhances delignification but reduces cellulose and xylan retention in pulp.

PC2 is primarily driven by ethanol concentration, as shown in the score plot (Figure 3B), while time shows no distinct trend along either axis. The loading plot further reveals this axis is strongly correlated with xylan behavior (X, XR and XBL), suggesting that ethanol provides a secondary, independent lever to control hemicellulose removal.

3.3 Fractionation at high severity (design B)

To explore a wide range of operating conditions, the experimental design was divided into two blocks. Responses may behave differently under low and high severity conditions, and a single large space could reduce statistical accuracy. Design A focused on low severity conditions to identify the two key factors affecting all responses: NaOH concentration and temperature. Design B extended the range to higher severities, focusing on these two factors to explore their effect on the chemical composition of the pulp and the performance of the fractionation process. This sequential approach can reduce experimental error and ensures reliable estimation of the effects of factors across the entire design space.

3.3.1 RSM-ANOVA

Table 7 summarizes the experimental runs with independent variables (temperature and NaOH concentration) and the dependent variables obtained, including the directly measured responses and performance indicators. ANOVA confirmed the significance and adequacy of the linear model for pulp yield (Y), cellulose content (C), residual xylan content (X), and xylan retention (XR); the quadratic model for cellulose retention (CR), residual lignin content (L), lignin removal (LR), and xylan in black liquor (XBL). Model equations and regression parameters for Design B are presented in Table 8. For all responses in Design B, the regression model was statistically significant ($p < 0.05$), and the F-values of LoF were insignificant, confirming that the models are adequate and that the residual variation can be attributed to random experimental error rather than an omitted systematic structure. The complete equation including all terms is presented in Supplementary Equations S9–S16. As observed in each term in the equations, two variables and their interaction affect all variables in the same direction. This indicates a synergetic effect from the two variables in the alkali-ethanol system at high severity. A full ANOVA for all terms is shown in Supplementary Table S2. Temperature and NaOH concentration are significant factors affecting all responses except xylan dissolution in liquid fraction.

3.3.2 Response surface

According to the ANOVA results, the significant factors affecting each response in Design B were visualized using linear, quadratic and three-dimensional response surface model (Figures 4, 5). For two-dimensional linear and quadratic plots, one factor was fixed at its midpoint while the other varied within its experimental range.

3.3.2.1 Pulp yield and chemical composition

Design B revealed linear trends for pulp yield (49.97%–59.50%), cellulose (62.53%–69.00%), and residual xylan (21.34%–25.57%)

10.3389/fceng.2026.1791044

TABLE 9 Optimization with desired goal in Design A and Design B and the experimental results.

Design A		Variables				Dependent variables							
		T (°C)	t (min)	NaOH (%)	EtOH (%)	Y (%)	C (%)	X (%)	L (%)	X_{BL} (mg)	CR (%)	XR (%)	LR (%)
A1	Goal 1	In range	In range	In range	In range	Max.	Max.	Max.	Min.	Min.	Max.	Max.	Max.
	Optimum	80	160	10.44	60	73.70	55.97	25.82	8.68	17.12	96.87	92.21	63.70
	Exp. Results	80	160	10.2	60	73.70	57.28	24.50	9.51	17.27	99.87	89.33	62.17
A2	Goal2	In range	In range	In range	In range	In range	Max.	In range	Min.	In range	Max.	Max.	Max.
	Optimum	140	65.22	13.15	0	62.59	63.15	24.02	4.49	152.9	93.74	73.67	83.06
	Exp. Results	140	65	12.8	0	63.76	62.62	23.94	5.60	130.0	94.44	75.51	80.71
Design B		Variables											
		T (°C)	t (min)	NaOH (%)	EtOH (%)	Y (%)	C (%)	X (%)	L (%)	X_{BL} (mg)	CR (%)	XR (%)	LR (%)
B1	Goal 1	In range	In range	In range	In range	Max.	Max.	Max.	Min.	Min.	Max.	Max.	Max.
	Optimum	169.2	110	16	30	57.58	64.69	24.38	3.58	155.6	88.16	62.58	88.94
	Exp. Results	169	110	16	30	57.72	65.09	23.67	4.35	131	88.88	67.58	86.46
B2	Goal2	In range	In range	In range	In range	In range	Max.	In range	Min.	In range	Max.	Max.	Max.
	Optimum	174.4	110	24	30	52.97	67.47	22.73	3.05	181.9	84.75	52.92	91.34
	Exp. Results	174	110	24	30	52.22	69.84	20.40	3.64	138.1	86.29	52.70	89.73

with respect to temperature and NaOH. Although no significant interaction was detected, both factors strongly affected the responses. Pulp yield decreased linearly with increasing temperature or NaOH concentration, while cellulose content increased correspondingly (Figure 4A). This indicates the progressive dissolution of non-cellulosic components as fractionation severity intensifies. Residual xylan content decreased more with increasing NaOH concentration than with temperature, suggesting that xylan was primarily affected by NaOH. Compared to cellulose and xylan contents, residual lignin content showed a more complex trend (Figure 4B). Values ranged narrowly between 3.07% and 4.19%, reflecting the limited variation within the high-severity range of Design B. Such small changes can influence model fitting and statistical accuracy. Lignin decreased with increasing temperature and NaOH, but at the high severity, a slight reversal occurred. This may indicate the aggregation of lignin fragments at high severity, resulting in the reabsorption of lignin into the pulp. This phenomenon was also suggested by Alves and Calado (Alves and Calado, 2025), who reported that high alkali concentrations and temperatures can induce aggregative and conformational changes of lignin in alkaline media.

3.3.2.2 Fractionation efficiency

Cellulose retention, xylan retention, and xylan content in black liquor were found to range from 81.57% to 88.34%, 47.49%–68.09%, and 148.69–186.95 mg, respectively. Cellulose retention was influenced by temperature, NaOH concentration, and quadratic effect of temperature, as reflected by the curvature in Figure 5A. Xylan retention exhibited linear dependence on both temperature and NaOH concentration. In contrast, xylan content in black liquor was significantly affected only by NaOH concentration and its quadratic term. Initially, with increasing NaOH concentration, xylan content increased, indicating enhanced solubilization from the pulp into the liquid fraction. However, beyond a certain level, xylan content decreased, suggesting xylan degradation *via* alkaline hydrolysis at higher alkalinity. Lignin removal ranged from 86.79% to 91.46%, confirming the overall high delignification under the severe conditions of Design B. As shown in Figure 5B, the response surface exhibits a similar curvature trend as observed for residual lignin content, reflecting the nonlinear influence of temperature and NaOH concentration.

3.3.3 Multivariate analysis

In the analysis of Design B, PC1 and PC2 together accounted for 92.3% of the total variance (79.6% and 12.7%, respectively). Due to the small number of runs (n = 11), the narrow operating range, and the lack of time and ethanol as factors, this PCA model is less robust and should be interpreted cautiously. Nevertheless, unlike Design A, the score plot for Design B (Figure 6A) shows that higher process intensity (higher temperature and NaOH concentration) corresponds to positive scores on the PC1 axis. This inversion of axis orientation arises from dataset scaling differences and does not alter the underlying interpretation. Temperature is the dominant

TABLE 10 Morphological properties of pulp obtained at four optima.

Sample	Mean length (mm)	Mean width (μm)	Slenderness ratio (SR)	Mean fibril perimeter (%)	FinesP (%)	FinesS (%)	Mean kink indexs
A1	0.51 ±0.03	27.03 ±0.93	18.76 ±0.56	5.37 ±1.00	17.20 ±6.42	68.83 ±12.95	2.35 ±0.12
A2	0.65 ±0.02	24.85 ±0.84	25.93 ±0.15	4.50 ±0.35	18.68 ±2.41	41.45 ±6.36	1.90 ±0.17
B1	0.68 ±0.01	23.47 ±0.29	29.02 ±0.66	4.57 ±0.55	21.23 ±1.16	19.60 ±4.08	1.98 ±0.04
B2	0.64 ±0.02	21.47 ±0.12	29.58 ±1.00	3.73 ±0.21	22.57 ±0.95	21.33 ±0.15	3.42 ±0.69

driver of PC1 and PC2 in Design B, while NaOH contributes similarly but with a weaker trend. The loading plot for Design B (Figure 6B) provides that yield (Y), residual xylan (X), lignin (L), cellulose retention (CR), and xylan retention (XR) are strongly correlated with the negative PC1 axis (lower process intensity). Conversely, conditions favoring high cellulose content (C), and lignin removal (LR) are found on the positive PC1 axis (higher process intensity). This again highlights the trade-off between delignification and carbohydrate preservation.

PC2, which is independent of the main severity trend of PC1, represents a subtle process optimization effect. This component is primarily characterized by a strong positive loading for xylan content in the black liquor (XBL) and, to a lesser extent, lignin content (L). This correlation suggests that PC2 identifies a specific process window within the high-severity region condition, xylan solubilization and delignification are maximized before extensive alkaline degradation of hemicellulose occurs.

3.4 Optimization of fractionation and morphological analysis of pulp

Based on the observed effects of operating variables on the responses and the interrelationships revealed by PCA, the correlative trends between responses were quantified. This analysis is particularly valuable for identifying the fundamental trade-offs of responses in process optimization. The strong negative correlations between certain responses, such as lignin removal *versus* xylan retention or pulp yield, indicate that these objectives act in opposition under the same operating conditions. Consequently, a single optimization target cannot effectively satisfy both goals. Therefore, two distinct optimization objectives were defined: 1. Maximizing pulp yield along with cellulose and xylan retention, and 2. Maximizing lignin removal while maintaining maximal cellulose retention. The numerical optimization of fractionation was performed by Design expert software by setting each desired optimization objectives for each response and the optimum was chosen by high desirability approach. Table 9 shows the calculated optima for both objectives in each design and the experimental results at these opima. The results demonstrated that relatively small errors with less than 5% for responses except residual lignin content in pulp, were measured. The relatively higher percentage error for residual lignin is attributed to the narrow experimental range of this response; when the absolute values are very small, even minor analytical variations result in a larger relative percentage, though the absolute difference remain statistically negligible.

To investigate the relationship between the variations in chemical composition achieved at the four optimized points (A1, A2, B1, and B2) and the resulting fiber morphology, a detailed morphological analysis was performed. These properties are critical as they influence pulp quality, papermaking performance, and the physical properties of the final bioproducts (Ferdous et al., 2021). While optimization objective 1 focused on carbohydrate retention and objective 2 aimed for maximum delignification *via* higher fractionation intensity. These chemical shifts, specifically the degree of lignin and hemicellulose removal, alter the structural integrity of the fiber wall, thereby influencing the physical dimensions and quality parameters.

The resulting morphological data, including length-weighted average length, width, Slenderness Ratio (SR), fibril perimeter, primary fines (FinesP), secondary fines (FinesS), and kink index are summarized in Table 10. The SR (length-to-width- ratio) is a key indicator of pulp digestibility and directly influences sheet density and tearing resistance (Agnihotri et al., 2010). Fibril perimeter serves as a proxy for the degree of external fibrillation, which is essential for inter-fiber hydrogen bonding and tensile strength development (Ferdous et al., 2021). To describe the fine material fraction, FinesP, originating from initial pulping, and FinesS, created during fiber development, were quantified. While higher fines content enhances sheet density and bonding strength, it can also reduce drainage and bleachability (Odabas et al., 2016; Fischer et al., 2017). Finally, the kink index provides insight into internal fiber stresses and flexibility, governing the bulk and stretch properties of the final paper (Ferdous et al., 2021). By correlating these parameters with process severity, this study characterizes the production of tailored fibers.

Fiber from Design A exhibited shorter mean length (0.51–0.65 mm) and larger mean width (24.85–27.03 μm), resulting in lower SR than fiber from Design B (length 0.64–0.68 mm; width 21.47–23.47 μm). The shorter length measured at low severity likely reflects incomplete fiber liberation from the biomass matrix, where residual lignin in the middle lamella prevents the full separation of individual fibers, leading the analyzer to record shorter, intact fiber bundles. A higher SR indicates longer, thinner, and more flexible fiber, which contribute to improved tearing resistance of paper sheet (Tsalagkas et al., 2021). The higher SR observed in Design B suggests that increasing process

TABLE 11 Alkali and Alkali-ethanol fractionation performance on *Miscanthus* and other non-wood lignocellulosic biomass.

Raw material	Fractionation condition			Pulp yield	Cellulose content	Delignification	References
	Temp.	Time	Reagents				
Miscanthus sinensis	100 °C	180 min	2% NaOH	54.7%	—	Residual Klason lignin = 7.3%	Iglesias et al. (1996)
Miscanthus sinensis	90 °C	90 min	7.5% NaOH 60% EtOH	—	58.2%	Residual lignin = 16.7%	Serrano et al. (2010)
Jute	175 °C	150 min	20% NaOH 50% EtOH	66%	—	Kappa Number = 29	Sahin (2003)
Arundo donax L. reed	140 °C	180 min	25% NaOH 40% EtOH	47.6%	31.2%	Residual lignin ≈ 3.5%	Shatalov and Pereira (2002)
Sugar cane Bagasse	195 °C	90 min	15% NaOH 25% EtOH	45%	69%	Kappa Number = 12	Carvalho et al. (2014)
Sugar cane straw	175 °C	90 min	10% NaOH 45% EtOH	43.9%	60.1%	Kappa Number = 12	Carvalho et al. (2014)
Cotton stalk	160 °C	60 min	10% NaOH 45% EtOH	41.5%	—	Kappa Number ≈ 49.3	Akgül and Tozluoglu (2010)
False banana (Ensete ventricosum)	140 °C	61 min	15% NaOH 46.4% EtOH	69.9%	—	Kappa Number = 4.9	Berhanu et al. (2018)
Miscanthus giganteus	80 °C	160 min	10.4% NaOH 60% EtOH	73.7%	56%	Residual lignin = 8.7%	This study: A1
	140 °C	65 min	13.2% NaOH 0% EtOH	62.6%	63.2%	Residual lignin = 4.5%	This study: A2

severity promoted delignification and partial removal of the middle lamella–composed mainly of lignin with only a few cellulosic fibrils - leading to better fiber separation and liberation of more elongated fiber. The narrower fiber width observed in Design B further suggests partial dissolution or peeling of outer wall layers, which typically accompanies high alkali exposure.

Design A pulps contained a higher fraction of secondary fines (FinesS = 41–69%) than Design B (FinesS = 19–21%). Since fiber were not subjected to further refining after pretreatment, the higher FinesS of Design A can be attributed to incomplete delignification and easier detachment of outer fibrillar material the fiber surface under mild conditions. Conversely, the strong alkaline environment in Design B likely resulted in more complete dissolution of amorphous polysaccharides (decreased cellulose crystallinity) and reduced fibrillation, leading to lower FinesS. FinesP showed a modest increase with increasing severity, which may result from fiber cutting or cell wall fragmentation under harsher conditions.

Fibrillation trends were further supported by the fibril perimeter (FP), defined as the ratio between the perimeter of fibrils attached to the fiber and the total fiber (Frias et al., 2024). Mild alkaline conditions are known to cause fiber swelling due to lignin-carbohydrate complex disruption (Choi et al., 2016; Ji et al., 2018). At low severity (A1), incomplete chemical separation and residual lignin–hemicellulose complexes likely caused surface swelling and roughness, yielding an apparently higher FP (5.37%) than the other samples. With increasing NaOH concentration and process severity, improved delignification and removal of outer wall components led to smoother fiber surfaces and lower FP, reaching the minimum in B2 (3.73%). Perez A.D. et al. similarly observed that the fibril perimeter decreases with increasing temperature during deep eutectic solvent pulping of spruce chips (Pérez et al., 2025).

The mean kink index did not show a consistent trend, although the notably higher value in B2 suggests that extreme chemical severity may induce local fiber damage or increased stiffness after extensive lignin removal.

The optimal condition for papermaking in the single stage fractionation was observed for sample B1, which produced pulp with a high SR of 29.02 while maintaining a low kink index of 1.98. In contrast, pulp A1 still contained considerable amounts of lignin and carbohydrates, with incomplete disruption of lignin–carbohydrate complexes leading to swollen fiber structures. Although not directly suitable for papermaking, such pulp could serve as a valuable intermediate for a second stage treatment under mild conditions to achieve further fractionation while retaining a high carbohydrate content, or for enzymatic digestion toward bio-based chemical or fermentation processes. Pulp A2, obtained under slightly more severe conditions, represents another promising starting material for secondary processing, offering lower lignin content yet still mild process severity and short reaction time. The corresponding pulping liquors are rich in solubilized lignin, making them suitable for recovery and valorization within an integrated biorefinery framework. This diversity of systematically identified optima highlights the potential of controlled process tuning to generate

tailored pulp and liquor streams for different end-use applications, from papermaking to biochemical conversion.

3.5 Discussion

The impact of ethanol addition to alkaline pulping appears to be biomass-dependent and further conditioned by the pulping severity applied. While ethanol-alkali systems have been reported to enhance delignification or selectivity in several studies - for instance in pine sawdust and other wood pulps - these effects vary with lignin structure and pulping severity (Schenck et al., 2013; Imlauer Vedoya et al., 2022). A lower kappa number and/or greater yield selection can be achieved in fiber crops and herbaceous materials by adding ethanol under certain conditions, but the magnitude depends on factors such as ethanol fraction, temperature, alkaline charge, and time (Sahin, 2003; Shatalov and Pereira, 2004; Berhanu et al., 2018). In the present study with *Miscanthus* × *giganteus*, carried out under low severity (Design A), ethanol did not exert a significant main effect on lignin removal, though an interactive effect with NaOH concentration was detected. It has been shown in several reports that Miscanthus lignin is characterized by a high syringyl-to-guaiacyl (S/G) ratio (Bauer et al., 2012; Kim and Um, 2020). The relatively high S/G ratio of Miscanthus lignin makes it more alkali-soluble due to fewer condensed C–C linkages and a higher proportion of cleavable β–O–4 ether bonds (Chen and Dixon, 2007; Li et al., 2016). Thus, alkali alone may be sufficient to delignify lignin efficiently at low severity, which is why ethanol addition was not significant in this study. In contrast, the addition of ethanol influenced hemicellulose dissolution, with higher ethanol concentrations reducing carbohydrate losses and thereby improving pulp yield in the studied condition range. While the current work focused on the effects of temperature and NaOH concentration at high severity, future investigations could evaluate the influence of varying ethanol concentration. This would help determine whether higher ethanol concentrations could mitigate extensive hemicellulose degradation, which is typically observed during high-intensity fractionation.

The optimized results from Design A (low severity) were compared with literature data on alkali- and alkali-ethanol fractionation of *Miscanthus* and various herbaceous feedstocks (Table 11). Although the chemical compositions and lignin structures of these biomass vary, alkali-ethanol fractionation consistently proves to be an effective fractionation strategy. Unlike previous studies seeking a single compromise between high delignification and yield, this study identified distinct operational optima tailored to specific biorefinery goals.

For the A1 optimum (polysaccharide yield focused), the process achieved a high yield of 73.7%, which is superior to the yields reported for the traditional alkali fractionation of *Miscanthus sinensis* (Iglesias et al., 1996). This outcome underscores the distinct role of ethanol in carbohydrate preservation. Furthermore, the pulp yield for the A1 optimum exceeded those of other studies. Although the cellulose content was lower than that observed in the fractionation sugarcane bagasse or straw (Carvalho et al., 2014), the higher overall pulp yield indicates significant hemicellulose retention. For the A2 optimum (delignification focused), a high degree of lignin removal was achieved, resulting in 4.5% residual lignin. These conditions were milder than those reported in other studies. For example, deep delignification of feedstocks such as jute, sugarcane bagasse, straw, and cotton stalk typically requires temperatures exceeding 160 °C (Sahin, 2003; Akgül and Tozluoglu, 2010; Carvalho et al., 2014) or high NaOH concentrations (e.g., 20%–25% for jute and reed) (Shatalov and Pereira, 2004). The fractionation conditions for false banana were found to be similar to the A2 optimum (Berhanu et al., 2018).

4 Conclusion

Alkali-ethanol fractionation of *Miscanthus* × *giganteus* was conducted using sequential Design of Experiments (DoE) with two experimental designs at different severity levels to systematically investigate the relationships between the process variables, pulp compositions and fractionation efficiency. Design A, representing low severity conditions, revealed the main drivers influencing pulp properties were alkali concentration and temperature, while ethanol primarily affected hemicellulose retention. For high severity conditions (Design B), alkali concentration and temperature exhibited synergistic effects on pulp properties as well as hemicellulose degradation in the liquid fractions and lignin aggregation at a high level of fractionation intensity. PCA further revealed that delignification counteracted pulp yield and carbohydrate retention, highlighting the trade-offs inherent in process optimization. Consequently, two optimization objectives were defined for each design: 1. Maximal pulp yield with carbohydrate retention and 2. Maximal delignification. Four distinct optima were derived based on the experimental designs, and validation experiments confirmed the adequacy of the model predictions.

This systematic approach not only clarified the relationships among the process, structure, and properties of products in alkaline-ethanol fractionation but also demonstrated how tuning operating conditions can produce pulps and liquors with distinct compositional characteristics. These findings provide a valuable foundation for developing multi-stage fractionation strategies and integrated biorefinery concepts, where specific product streams can be optimized for papermaking, lignin recovery, or carbohydrate-based bioconversion.

Data availability statement

The original contributions presented in the study are included in the article/Supplementary Material, further inquiries can be directed to the corresponding author.

Author contributions

HC: Investigation, Visualization, Writing – review and editing, Methodology, Writing – original draft. NC: Conceptualization, Supervision, Writing – review and editing, Methodology, Project

administration. MD: Writing – review and editing, Supervision, Conceptualization, Funding acquisition. RP: Writing – review and editing, Resources. HK: Methodology, Writing – review and editing, Supervision, Conceptualization. AJ: Writing – review and editing, Supervision, Funding acquisition.

Funding

The author(s) declared that financial support was received for this work and/or its publication. This project, IN-FIBRE, was performed as part of the Bioeconomy Science Center (BioSC), supported by Marga und Walter Boll-Stiftung.

Acknowledgements

The authors thank Axel Wizemann for his support, as well as Laura Beust from Modellfabrik Papier gGmbH for providing access to the fiberanalyzer.

Conflict of interest

The author(s) declared that this work was conducted in the absence of any commercial or financial relationships that could be construed as a potential conflict of interest.

Generative AI statement

The author(s) declared that generative AI was used in the creation of this manuscript. During the preparation of this manuscript, the quthor used generative AI to help edit manuscript for languages clarity.

Any alternative text (alt text) provided alongside figures in this article has been generated by Frontiers with the support of artificial intelligence and reasonable efforts have been made to ensure accuracy, including review by the authors wherever possible. If you identify any issues, please contact us.

Publisher's note

All claims expressed in this article are solely those of the authors and do not necessarily represent those of their affiliated organizations, or those of the publisher, the editors and the reviewers. Any product that may be evaluated in this article, or claim that may be made by its manufacturer, is not guaranteed or endorsed by the publisher.

Supplementary material

The Supplementary Material for this article can be found online at: https://www.frontiersin.org/articles/10.3389/fceng.2026.1791044/full#supplementary-material

References

Agnihotri, S., Dutt, D., and Tyagi, C. H. (2010). Complete characterization of bagasse of early species of Saccharum officinerum-co 89003 for pulp and paper making. *BioResources* 5 (2), 1197–1214. doi:10.15376/biores.5.2.1197-1214

Akgül, M., and Tozluoglu, A. (2010). Alkaline-ethanol pulping of cotton stalks. *Sci. Res. Essays* 5 (10), 1068–1074. doi:10.5897/SRE.9000144

Aklilu, E. G. (2020). Optimization and modeling of ethanol-alkali pulping process of bamboo (*Yushania alpina*) by response surface methodology. *Wood Sci. Technol.* 54 (5), 1319–1347. doi:10.1007/s00226-020-01188-z

Alves, A. L., and Calado, V. (2025). An empirical assessment of the physicochemical properties of lignin solutions in aqueous sodium hydroxide - corroboration and demystification of some widely accepted statements. *Faraday Discuss.* 263, 319–335. doi:10.1039/d5fd00071h

Bauer, S., Sorek, H., Mitchell, V. D., Ibáñez, A. B., and Wemmer, D. E. (2012). Characterization of *Miscanthus giganteus* lignin isolated by ethanol organosolv process under reflux condition. *J. Agric. Food Chem.* 60 (33), 8203–8212. doi:10.1021/jf302409d

Ben Fradj, N., Rozakis, S., Borzęcka, M., and Matyka, M. (2020). Miscanthus in the European bio-economy: a network analysis. *Indust. Crops Prod.* 148, 112281. doi:10.1016/j.indcrop.2020.112281

Bergs, M., Do, X. T., Rumpf, J., Kusch, P., Monakhova, Y., Konow, C., et al. (2020). Comparing chemical composition and lignin structure of *Miscanthus x giganteus* and *Miscanthus nagara* harvested in autumn and spring and separated into stems and leaves. *RSC Adv.* 10 (18), 10740–10751. doi:10.1039/c9ra10576j

Bergs, M., Monakhova, Y., Diehl, B. W., Konow, C., Völkering, G., Pude, R., et al. (2021). Lignins isolated *via* catalyst-free organosolv pulping from Miscanthus x giganteus. A Comparative study. *Mol. (Basel, Switz.)* 26 (4), 842. doi:10.3390/molecules26040842

Berhanu, H., Kiflie, Z., Neiva, D., Gominho, J., Feleke, S., Yimam, A., et al. (2018). Optimization of ethanol-alkali delignification of false banana (*Ensete ventricosum*) fibers for pulp production using response surface methodology. *Industrial Crops Prod.* 126, 426–433. doi:10.1016/j.indcrop.2018.08.093

Biermann, C. J. (1993). *Essentials of pulping and papermaking*. San Diego: Academic Press.

Brosse, N., Sannigrahi, P., and Ragauskas, A. (2009). Pretreatment of *Miscanthus x giganteus* using the ethanol organosolv process for ethanol production. *Industrial Eng. Chem. Res.* 48 (18), 8328–8334. doi:10.1021/ie9006672

Carvalho, D.M. von, Magalhães, W., Pérez, D. S., Queda, F., and Pereira, H. (2014). Ethanol-soda pulping of sugarcane bagasse and straw. *Cellul. Chem. Technol.* 48 (3-4), 355–364.

Chen, F., and Dixon, R. A. (2007). Lignin modification improves fermentable sugar yields for biofuel production. *Nat. Biotechnol.* 25 (7), 759–761. doi:10.1038/nbt1316

Choi, K.-H., Kim, A. R., and Cho, B.-U. (2016). Effects of alkali swelling and beating treatments on properties of kraft pulp fibers. *BioResources* 11 (2), 3769–3782. doi:10.15376/biores.11.2.3769-3782

Clifton-Brown, J., Hastings, A., Mos, M., McCalmont, J. P., Ashman, C., Awty-Carroll, D., et al. (2017). Progress in upscaling *Miscanthus* biomass production for the European bio-economy with seed-based hybrids. *GCB Bioenergy* 9 (1), 6–17. doi:10.1111/gcbb.12357

Czyrski, A., and Jarzębski, H. (2020). Response surface methodology as a useful tool for evaluation of the recovery of the fluoroquinolones from plasma—the study on applicability of box-behnken design, central composite design and doehlert design. *Processes* 8 (4), 473. doi:10.3390/pr8040473

Da Costa, R. M. F., Pattathil, S., Avci, U., Lee, S. J., Hazen, S. P., Winters, A., et al. (2017). A cell wall reference profile for miscanthus bioenergy crops highlights compositional and structural variations associated with development and organ origin. *New Phytologist* 213 (4), 1710–1725. doi:10.1111/nph.14306

Dagnino, E. P., Felissia, F. E., Chamorro, E., and Area, M. C. (2017). Optimization of the soda-ethanol delignification stage for a rice husk biorefinery. *Industr. Crops Prod.* 97, 156–165. doi:10.1016/j.indcrop.2016.12.016

Danielewicz, D., and Surma-Ślusarska, B. (2019). *Miscanthus* × *giganteus* stalks as a potential non-wood raw material for the pulp and paper industry. Influence of pulping and beating conditions on the fibre and paper properties. *Industrial Crops Prod.* 141, 111744. doi:10.1016/j.indcrop.2019.111744

Danielewicz, D., Surma-Ślusarska, B., Żurek, G., Martyniak, D., Kmiotek, M., and Dybka, K. (2015). Selected grass plants as biomass fuels and raw materials for papermaking, part II. Pulp and paper properties. *BioResources* 10 (4), 8552–8564. doi:10.15376/biores.10.4.8552-8564

Fardim, P., and Durán, N. (2004). Retention of cellulose, xylan and lignin in kraft pulping of eucalyptus studied by multivariate data analysis: influences on physicochemical and mechanical properties of pulp. *J. Braz. Chem. Soc.* 15 (4), 514–522. doi:10.1590/S0103-50532004000400012

Ferdous, T., Ni, Y., Quaiyyum, M. A., Uddin, M. N., and Jahan, M. S. (2021). Non-wood fibers: relationships of fiber properties with pulp properties. *ACS Omega* 6 (33), 21613–21622. doi:10.1021/acsomega.1c02933

Fischer, W. J., Mayr, M., Spirk, S., Reishofer, D., Jagiello, L. A., Schmiedt, R., et al. (2017). Pulp fines-characterization, sheet formation, and comparison to microfibrillated cellulose. *Polymers* 9 (8), 1–12. doi:10.3390/polym9080366

Food and Agriculture Organization of the United Nations (2024). *Global forest products facts and figures 2023*. Available online at: https://openknowledge.fao.org (Accessed August 22, 2025).

Frias, J.A. de, and Feng, H. (2013). Switchable butadiene sulfone pretreatment of *Miscanthus* in the presence of water. *Green Chem.* 15 (4), 1067. doi:10.1039/c3gc37099b

Frias, M., Reynoso, S., Rambhia, S., Noki, G., Olson, J., Stoeber, B., et al. (2024). Effect of incubation conditions of cellulase hydrolysis on mechanical pulp fibre morphology. *Carbohydr. Polym.* 344, 122529. doi:10.1016/j.carbpol.2024.122529

Gismatulina, Y. A., Budaeva, V. V., Kortusov, A. N., Kashcheyeva, E. I., Gladysheva, E. K., Mironova, G. F., et al. (2022). Evaluation of chemical composition of *Miscanthus* × *giganteus* raised in different climate regions in Russia. *Plants (Basel, Switz.)* 11 (20), 2791. doi:10.3390/plants11202791

He, L., Chen, D., Yang, S., Peng, L., Zhang, J., Guan, Q., et al. (2020). Deep insights into the atmospheric sodium hydroxide–hydrogen peroxide extraction process of Hemicellulose in Bagasse pith: technical uncertainty, dissolution kinetics behavior, and mechanism. *Industrial Eng. Chem. Res.* 59 (21), 10150–10159. doi:10.1021/acs.iecr.0c01076

Iglesias, G., Bao, M., Lamas, J., and Vega, A. (1996). Soda pulping of *Miscanthus sinensis*. Effects of operational variables on pulp yield and lignin solubilization. *Bioresour. Technol.* 58 (1), 17–23. doi:10.1016/S0960-8524(96)00087-9

Imlauer Vedoya, C. M., Area, M. C., Raffaeli, N., and Felissia, F. E. (2022). Study on soda–ethanol delignification of pine sawdust for a biorefinery. *Sustainability* 14 (11), 6660. doi:10.3390/su14116660

Ji, Y., Peng, Y., Strand, A., Fu, S., Sundberg, A., and Retulainen, E. A. (2018). Fiber evolution during alkaline treatment and its impact on handsheet properties. *BioResources* 13 (4), 7310–7324. doi:10.15376/biores.13.4.7310-7324

Kim, G.-H., and Um, B.-H. (2020). Fractionation and characterization of lignins from *Miscanthus via* organosolv and soda pulping for biorefinery applications. *Int. J. Biol. Macromol.* 158, 443–451. doi:10.1016/j.ijbiomac.2020.04.229

Lan, K., Xu, Y., Kim, H., Ham, C., Kelley, S. S., and Park, S. (2021). Techno-economic analysis of producing xylo-oligosaccharides and cellulose microfibers from lignocellulosic biomass. *Bioresour. Technol.* 340, 125726. doi:10.1016/j.biortech.2021.125726

Lee, W.-C., and Kuan, W.-C. (2015). Miscanthus as cellulosic biomass for bioethanol production. *Biotechnol. J.* 10 (6), 840–854. doi:10.1002/biot.201400704

Lemma, H. B., Freund, C., Yimam, A., Steffen, F., and Saake, B. (2023). Prehydrolysis soda pulping of Enset fiber for production of dissolving grade pulp and biogas. *RSC Adv.* 13 (7), 4314–4323. doi:10.1039/d2ra07220c

Li, M., Pu, Y., and Ragauskas, A. J. (2016). Current understanding of the correlation of lignin structure with biomass recalcitrance. *Front. Chem.* 4, 45. doi:10.3389/fchem.2016.00045

Li, P., Xu, Y., Yin, L., Liang, X., Wang, R., and Liu, K. (2023). Development of raw materials and technology for Pulping-A brief review. *Polymers* 15 (22), 4465. doi:10.3390/polym15224465

Mohamad, N. A. N., and Jai, J. (2022). Response surface methodology for optimization of cellulose extraction from banana stem using NaOH-EDTA for pulp and papermaking. *Heliyon* 8 (3), e09114. doi:10.1016/j.heliyon.2022.e09114

Moll, L., Wever, C., Völkering, G., and Pude, R. (2020). Increase of miscanthus cultivation with new roles in materials Production—A review. *Agronomy* 10 (2), 308. doi:10.3390/agronomy10020308

Montgomery, D. C. (2017). *Design and analysis of experiments*. 9th edition. Hoboken, NJ: John Wiley and Sons.

Muniz Kubota, A., Kalnins, R., and Overton, T. W. (2018). A biorefinery approach for fractionation of Miscanthus lignocellulose using subcritical water extraction and a modified organosolv process. *Biomass Bioenergy* 111, 52–59. doi:10.1016/j.biombioe.2018.01.019

Myers, R. H., Montgomery, D. C., and Anderson-Cook, C. M. (2016). *Response surface methodology: process and product optimization using designed experiments*. 4th edition. Hoboken, New Jersey: John Wiley & Sons, Inc.

Ngan, C. L., Basri, M., Lye, F. F., Fard Masoumi, H. R., Tripathy, M., Abedi Karjiban, R., et al. (2014). Comparison of Box–Behnken and central composite designs in optimization of fullerene loaded palm-based nano-emulsions for cosmeceutical application. *Industrial Crops Prod.* 59, 309–317. doi:10.1016/j.indcrop.2014.05.042

Odabas, N., Henniges, U., Potthast, A., and Rosenau, T. (2016). Cellulosic fines: properties and effects. *Prog. Mater. Sci.* 83, 574–594. doi:10.1016/j.pmatsci.2016.07.006

Oza, S., Kodgire, P., and Kachhwaha, S. S. (2022). Analysis of RSM based BBD and CCD techniques applied for biodiesel production from waste cotton-seed cooking oil *via* ultrasound method. *Anal. Chem. Lett.* 12 (1), 86–101. doi:10.1080/22297928.2021.2019611

Peng, X., Nie, S., Li, X., Huang, X., and Li, Q. (2019). Characteristics of the Water- and alkali-soluble hemicelluloses fractionated by sequential acidification and graded-ethanol from sweet maize stems. *Mol. (Basel, Switz.)* 24 (1), 1–9. doi:10.3390/molecules24010212

Pérez, A. D., Roy, Y., Rip, C., Kersten, S. R. A., and Schuur, B. (2025). Influence of pulping conditions on the pulp yield and fiber properties for pulping of spruce chips by deep eutectic solvent. *Biomass Convers. Biorefinery* 15 (1), 1377–1391. doi:10.1007/s13399-023-05156-y

Rivas, S., Santos, V., and Parajó, J. C. (2022). Effects of hydrothermal processing on *Miscanthus* × *giganteus* polysaccharides: a kinetic assessment. *Polymers* 14 (21), 4732. doi:10.3390/polym14214732

Sahin, H. T. (2003). Base-catalyzed organosolv pulping of jute. *J. Chem. Technol. Biotechnol.* 78 (12), 1267–1273. doi:10.1002/jctb.931

Sahin, H. T., and Young, R. A. (2008). Auto-catalyzed acetic acid pulping of jute. *Industrial Crops Prod.* 28 (1), 24–28. doi:10.1016/j.indcrop.2007.12.008

Schäfer, J., Sattler, M., Iqbal, Y., Lewandowski, I., and Bunzel, M. (2019). Characterization of *Miscanthus* cell wall polymers. *Glob. Change Biol. Bioenergy* 11 (1), 191–205. doi:10.1111/gcbb.12538

Schenck, A. von, Berglin, N., and Uusitalo, J. (2013). Ethanol from Nordic wood raw material by simplified alkaline soda cooking pre-treatment. *Appl. Energy* 102, 229–240. doi:10.1016/j.apenergy.2012.10.003

Serrano, L., Egües, I., Alriols, M. G., Llano-Ponte, R., and Labidi, J. (2010). Miscanthus sinensis fractionation by different reagents. *Chem. Eng. J.* 156 (1), 49–55. doi:10.1016/j.cej.2009.09.032

Shakhes, J., Zeinaly, F., Marandi, M. a., and Saghafi, T. (2011). The effects of processing variables on the soda and soda-AQ pulping of kenaf bast fiber. *BioResources* 6 (4), 4626–4639. doi:10.15376/biores.6.4.4626-4639

Shatalov, A. (2002). Carbohydrate behaviour of *Arundo donax* L. in ethanol–alkali medium of variable composition during organosolv delignification. *Carbohydr. Polym.* 49 (3), 331–336. doi:10.1016/S0144-8617(01)00340-X

Shatalov, A. A., and Pereira, H. (2002). Ethanol-enhanced alkaline pulping of *Arundo donax* L. Reed: influence of solvent on pulp yield and quality. *Holzforschung* 56 (5), 507–512. doi:10.1515/HF.2002.078

Shatalov, A., and Pereira, H. (2004). *Arundo donax* L. reed: new perspectives for pulping and bleaching, Part 3: ethanol reinforced alkaline pulping. *TAPPI J.* 3 (2), 27–31.

Shepherd, A., Awty-Carroll, D., Kam, J., Ashman, C., Magenau, E., Martani, E., et al. (2023). Novel Miscanthus hybrids: modelling productivity on marginal land in Europe using dynamics of canopy development determined by light interception. *Glob. Change Biol. Bioenergy* 15 (4), 444–461. doi:10.1111/gcbb.13029

Sjöström, E. (1977). The behavior of wood polysaccharides during alkaline pulping processes, 60(9), 151–154.

Sjöström, E. (1991). Carbohydrate degradation products from alkaline treatment of biomass. *Biomass Bioenergy* 1 (1), 61–64. doi:10.1016/0961-9534(91)90053-F

Sluiter, A., Ruiz, R., Scarlata, C., Sluiter, J., and Templeton, D. (2005a). *Determination of ash in biomass: laboratory Analytical Procedure (LAP)*. Golden, CO. Available online at: https://NREL/TP-510-42622.nrel.gov (Accessed October 20, 2024).

Sluiter, A., Ruiz, R., Scarlata, C., Sluiter, J., and Templeton, D. (2005b). *Determination of extractives in biomass: laboratory Analytical Procedure (LAP)*. Golden, CO. Available online at: https://NREL/TP-510-42619:nrel.gov (Accessed October 20, 2024).

Sluiter, A., Hyman, D., Payne, C., Ruiz, R., Scarlata, C., Sluiter, J., et al. (2006). *Determination of sugars, byproducts, and degradation products in liquid fraction process samples: laboratory Analytical Procedure (LAP); issue date: 12/08/2006*. Golden, CO. Available online at: https://NREL/TP-510-42623:nrel.gov (Accessed October 12, 2024).

Sluiter, A., Hames, B., Ruiz, R., Scarlata, C., Sluiter, J., Templeton, D., et al. (2012). *Determination of Structural Carbohydrates and Lignin in Biomass: Laboratory Analytical Procedure (LAP) (Revised July 2011)*. Golden, CO. Available online at: https://NREL/TP-510-42618:nrel.gov (Accessed October 12, 2024).

Takada, M., Chandra, R., Wu, J., and Saddler, J. N. (2020). The influence of lignin on the effectiveness of using a chemithermomechanical pulping based process to pretreat softwood chips and pellets prior to enzymatic hydrolysis. *Bioresour. Technol.* 302, 122895. doi:10.1016/j.biortech.2020.122895

Tayyab, M. (2018). Bioethanol production from Lignocellulosic Biomass by environment-friendly pretreatment methods: a review. *Appl. Ecol. Environ. Res.* 16 (1), 225–249. doi:10.15666/aeer/1601_225249

Thykesson, M., Sjöberg, L.-A., and Ahlgren, P. (1998). Paper properties of grass and straw pulps. *Industrial Crops Prod.* 7 (2-3), 351–362. doi:10.1016/S0926-6690(97)10001-2

Tsalagkas, D., Börcsök, Z., Pásztory, Z., Gryc, V., Csóka, L., and Giagli, K. (2021). A comparative fiber morphological analysis of major agricultural residues (used or investigated) as feedstock in the pulp and paper industry. *BioResources* 16 (4), 7935–7952. doi:10.15376/biores.16.4.7935-7952

Wang, K., Bauer, S., and Sun, R. (2012). Structural transformation of *Miscanthus* × *giganteus* lignin fractionated under mild formosolv, basic organosolv, and cellulolytic enzyme conditions. *J. Agric. Food Chem.* 60 (1), 144–152. doi:10.1021/jf2037399

Xu, C., Liu, F., Alam, M. A., Chen, H., Zhang, Y., Liang, C., et al. (2020). Comparative study on the properties of lignin isolated from different pretreated sugarcane bagasse and its inhibitory effects on enzymatic hydrolysis. *Int. J. Biol. Macromol.* 146, 132–140. doi:10.1016/j.ijbiomac.2019.12.270

Zhang, H., and Wu, S. (2014). Efficient sugar release by acetic acid ethanol-based organosolv pretreatment and enzymatic saccharification. *J. Agric. Food Chem.* 62 (48), 11681–11687. doi:10.1021/jf503386b